Lecture Notes for NSF-APS DPP GPAP 2021 Summer School

Kristopher G. Klein

Department of Planetary Sciences, University of Arizona, Tucson, AZ 85719, USA

Lunar and Planetary Laboratory, University of Arizona, Tucson, AZ 85719, USA

(compiled on 4 June 2021)

The purpose of these notes is provide additional background and details on the lectures presented by Prof. Klein at the National Science Foundation American Physics Society Division of Plasma Physics Topical Group in Plasma Astrophysics (GPAP) 2021 Summer School. The two specific topics under consideration are:

CONTENTS

Caveat lector, typographical error likely abound through this text. They will be corrected, and this document updated, as they are brought to the author's attention.

PART I
Turbulence

How easy a thing is it for a man to put off from him all turbulent adventitious imaginations, and presently to be in perfect rest and tranquility!

Meditations Book V
Marcus Aurelius
trans. J. Boulton

I.1. Fluid Turbulence

We turn to the study of multiscale disorder, and the accompanying nonlinear transfer of energy between structures with different scale sizes, known generally as turbulence.

In this lecture, we focus on introducing basic turbulence concepts, and identifying how these processes are affected by the introduction of magnetic fields and charged particles.

I.1.1. *Why Do We Care About Turbulence?*

Turbulence is ubiquitous[1], arising in many terrestrial, solar, and astrophysical environments. For example, turbulence plays a significant role in

- Laboratory Fusion Devices, (Dimits et al. 2000)
- Solar Wind and Solar Corona (Cranmer et al. 2007; Bruno and Carbone 2013)
- The Interstellar Medium (Armstrong et al. 1995)
- The Solar Interior (Kim 2005)
- Accretion Disks (Kunz et al. 2016)
- Galaxy Clusters (Zhuravleva et al. 2014)

Apart from being intrinsically interesting, turbulence plays an important role in plasmas by governing the transport of

- Mass— leading to loss of confinement in laboratory devices, mixing and accretion of matter.
- Momentum— infall of accretion disk material and behavior near collisionless shocks and jets.
- Energy— channeling energy flow and determining how a plasma is heated.

As an example, consider the Magneto-Rotational Instability (MRI) in an accretion disk around a black hole (Balbus and Hawley 1998). This instability taps *free energy* in Keplerian differential rotation to drive turbulence at large scales. Angular momentum is transported outwards, allowing mass to fall inwards and accrete. Energy released as the matter falls into the gravitational potential well also powers the turbulence. A nonlinear cascade transfers this energy from larger to ever smaller length scales. At characteristic kinetic length scales, wave-particle interactions, e.g. Landau damping or cyclotron damping or magnetic reconnection, act to transfer electromagnetic energy the charged particles. This energy is irreversibly converted into plasma heat by the process of collisional relaxation. This hot plasma radiates away some of its heat, allowing us to see the accretion disk from Earth.

In addition to understanding the transfer of mass, momentum, and energy, turbulence also sets the background properties of fields and flows that very energetic particles must pass through. Having accurate models of turbulence is therefore essential for accurately modeling the transport of cosmic rays and solar energetic particles.

[1] As is the word 'ubiquitous' in the introduction of turbulence papers.

In the following section, we will focus primarily on the cascade of turbulence, in particular on the length scales smaller than where energy is injected into the system but larger than where the energy is removed by damping or dissipation. These intermediate scales, unaffected by driving or dissipation, are known as the *inertial range*.

I.1.2. *Kolmogorov's Theory of Fluid Turbulence*

Before diving into the theory of hydrodynamic turbulence proposed by Kolmogorov (1941), let us consider two complementary systems, a cup of coffee and a can of paint. If we add some cream to the coffee, or some color to the paint, and stir a few times, the mixing of the added elements will be very different. With those few short stirrings in the coffee, the cream rapidly mixes in, while the paint color is not well mixed at all. The difference is due to turbulence; flows in the coffee are turbulent, while flows in paint are laminar. We can make a more quantitative statement by comparing terms in the *Navier-Stokes* Equation,

$$\rho\frac{\partial \boldsymbol{U}}{\partial t} + \rho\boldsymbol{U}\cdot\nabla\boldsymbol{U} = -\nabla p + \mu\nabla^2\boldsymbol{U} \tag{I.1}$$

which describes the evolution of a neutral fluid. There are two terms on the right hand side of the equation that affect the evolution of the convected flow; the gradient of the pressure and the viscous term. The strength of the later term is proportional to μ, the coefficient of shear viscosity.

To characterize the relative rates at which the momentum is convected or diffused via viscosity, we define the ratio

$$\mathrm{R}_e \equiv \frac{|\boldsymbol{U}\cdot\nabla\boldsymbol{U}|}{\nu\nabla^2\boldsymbol{U}} \sim \frac{v_0^2/L}{\nu v_0/L^2} \sim \frac{Lv_0}{\nu}, \tag{I.2}$$

where $\nu = \mu/\rho$. This value, the **Reynolds number**, quantifies how easy is is for particles to move around compared to how quickly momentum is diffused by viscosity; when this ratio is small, viscosity is faster than the convection and we have laminar flows. When this ratio is large, the viscosity is slower than the convection and we have turbulent flows.

But, what does the turbulence do in high-Reynolds number systems? Consider the stirring of the coffee. Energy is injected at the largest size in the system, the size of the cup. This is the driving scale. Nonlinear interactions lead to a transfer of energy from the driving scale to smaller scales, forming eddies that are smaller than the size of the cup. These smaller fluctuations interact one with another, nonlinearly transfering their energy to even smaller scales. Eventually, these whorls are small enough that instead of continuing to cascade their energy to smaller fluctuations, viscosity acts to dissipate the energy, shutting off the cascade; in plasma systems, the mechanisms that terminate the cascade are not always clearly identified, and may vary depending on the plasma conditions, c.f. Chen et al. (2014).

Turning to a more formal treatment, Kolmogorov (1941) laid out the hypothesis that the energy transfer is **local** and that the energy cascade rate through the inertial range is constant, and in doing so was able to derive a set of scaling laws from these assumptions.

By a local transfer of energy, we mean that the energy transfer is dominated by interactions between eddies of similar scales, e.g. from scale l to $l/2$ not from l to $l/16$.

By invoking a constant cascade rate as a function of scale, we are effectively assuming a steady state solution. If the cascade where not constant, then energy would either build up or diminish at some scale and we would not have a steady state solution.

We define a 'eddy turn around' time scale τ[2] such that

$$\tau \sim \frac{l}{v} \tag{I.3}$$

where l is the size scale of the eddy and v is the speed of the whorl.

If we assume the energy at scale l is transferred to a smaller scale $l/2$ over the eddy turn around time τ, than the energy cascade rate ϵ will simply be

$$\epsilon = \frac{\text{energy}}{\text{time}} \sim \frac{v^2}{\tau} \sim \frac{v^3}{l}, \tag{I.4}$$

where we have assumed an incompressible fluid, so $\rho = \rho_0$, allowing us to write the kinetic energy per unit volume as

$$E = \frac{1}{2}\rho_0 v^2 \sim v^2 \tag{I.5}$$

since the mass density will always be the same.

As we have stipulated a constant cascade rate $\epsilon = \epsilon_0 = v^3/l$, we find the velocity of the eddy will scale with the size of the eddy as

$$v_l \sim \epsilon_0^{1/3} l^{1/3}, \tag{I.6}$$

where for notational convience, we have written $v_l = v(l)$.

Given this behavior, how will energy be distributed as a function of scale?

We define a (one-dimensional[3]) *Energy Spectrum* $E(k)$ (or equivalently E_k) such that

$$E = \int_k^\infty E(k)dk. \tag{I.7}$$

This definition implies that E_k has units of $\left[\frac{E}{k}\right]$. We can study turbulence by calculating, or measuring, this distribution of energy as a function of scale.

We remind the reader that the wavenumber l associated with a particular scale is $k = 2\pi/l \sim 1/l$.

Generally, self-similar physics yields power law behavior, which shows up as a straight-line on a log-log plot of E_k. The inertial range, bookended by the driving scale L and viscous scale l_ν, are the set of scales far from where energy is injected into the system and the scales where it is removed. One of the most straight forward ways of characterizing the nature of the turbulence is to measure, or predict, the spectral slope p of the power-law distribution $E_k \propto k^p$. For a Kolmogorov spectrum,

$$E_k \propto \frac{v_k^2}{k} \sim \frac{\epsilon_0^{2/3} k^{-2/3}}{k} \sim \epsilon_0^{2/3} k^{-5/3}. \tag{I.8}$$

Note that the cascade time decreases with scale

$$\tau_k \sim \frac{1}{k v_k} \sim \frac{1}{k(\epsilon_0^{2/3} k^{-2/3})} \sim k^{-2/3}. \tag{I.9}$$

This is why it only takes a couple stirring periods at the large scale for the energy to reach the viscous scale—why your cream mixes into your coffee quickly!

[2]In these scaling arguments, factors of order unity such as π are dropped.

[3]Note that generally energy is a function of three spatial dimensiones, and thus a full description of the energy distribution is given by $E^{(3)}(k_x, k_y, k_z)$. If this three-dimensional spectrum is isotropic in $\boldsymbol{k}$ space, we can use spherical coördinates to write $E = \int\int\int k^2 dk \sin\theta d\theta d\phi E^{(3)}$. Integrating over ϕ and θ, we are left with $E = \int k^2 dk E^{(3)} = \int dk E^{(1)}$, where $E^{(3)}$ is the one-dimensional spectrum.

Let's test how realistic our assumption of the 'local' transfer of energy is; in other words, Can big eddies shear apart small eddies before they cascade? Can small eddies diffuse the fluid across a larger eddy in a big eddy cascade time?

To tackle the first question, if we write the momentum equation

$$\rho\left[\frac{\partial \boldsymbol{U}}{\partial t}+\boldsymbol{U}\cdot\nabla\boldsymbol{U}=-\nabla P\right] \tag{I.10}$$

and Fourier transform in space and time, assuming a plane-wave like solution, we have

$$\omega\boldsymbol{U}-(\boldsymbol{k}\cdot\boldsymbol{U})\,\boldsymbol{U}=\frac{\boldsymbol{k}p}{\rho} \tag{I.11}$$

where ω is the linear frequency of evolution and $\boldsymbol{k}\cdot\boldsymbol{U}\sim kv$ is the eddy turnaround frequency (also known as the nonlinear frequency).

Assuming some large scale eddy has length L, velocity v_0, and a shearing rate of $v_0/L\sim k_0v_0\sim\omega_0$, we can estimate

$$\frac{\omega_0}{\omega}=\frac{k_0v_0}{kv_k}=\frac{k_0v_0}{k\left[v_0\left(\frac{k_0}{k}\right)^{1/3}\right]}=\left(\frac{k_0}{k}\right)^{2/3}\ll 1 \tag{I.12}$$

and therefore the shearing is too slow compared to the rate at which energy is transfered locally.

To tackle the 2nd question, we write down the diffusion coefficient due to an eddy of size $l\sim 1/k$

$$D_k=\frac{l^2}{\tau_l}=\frac{\omega_k}{k^2}=\frac{kv_k}{k^2}=\frac{v_k}{k} \tag{I.13}$$

The time to diffuse a larger distance $L\sim\frac{1}{k_0}$ is

$$\tau_D=\frac{L^2}{D_k}=\frac{1}{k_0^2D_k}\sim\frac{1}{\omega_D}. \tag{I.14}$$

Thus $\omega_D\sim k_0^2D_k=k_0^2\frac{v_k}{k}=kv_k\left(\frac{k_0}{k}\right)^2$.

Comparing this frequency to the eddy frequency at large scale $\omega=k_0v_0$ yields

$$\frac{\omega_D}{\omega_0}=\frac{kv_k}{k_0v_k}\left(\frac{k_0}{k}\right)^2=\frac{v_k}{v_k}\left(\frac{k_0}{k}\right)^{1/3}\left(\frac{k_0}{k}\right)=\left(\frac{k_0}{k}\right)^{4/3}\ll 1 \tag{I.15}$$

we see that this diffusion process is slow when k and k_0 do not have similar values.

Thus, it is the shearing and diffusion due to the local in scale size eddies with $k\sim k_0$ that dominate energy transfer from eddies at k_0 to smaller scales, as asserted by Kolmogorov.

In the next section, we will make things more complicated by adding in the effects of a magnetic field, which will organize how the structures can interact and will direct the transfer of energy into an anisotropy distribution.

Recommended Reading:

- Frisch (1995) is a good textbook length introduction to (mostly fluid) turbulence.
- Batchelor (1953) is a quality historical text that contains useful physical insight into fluid turbulence.

Big whorls have little whorls Which feed on their velocity,
And little whorls have lesser whorls And so on to viscosity.
Lewis Fry Richardson

I.2. MHD Turbulence

In the section on fluid turbulence, we focused on the nonlinear transport of energy in a fluid system at ranges well separated from the driving and dissipation scales. We will now complicate that picture by adding in the effects of a background magnetic field, and develop a theory of MHD turbulence.

The focus of today's lecture will be:

- Iroshnikov-Kraichan Theory of MHD Turbulence
- Weak MHD Turbulence
- Strong MHD Turbulence

I.2.1. *Iroshnikov-Kraichan Theory of MHD Turbulence*

Our first break from the fluid case follows in the footsteps of two complementary papers, Iroshnikov (1964) and Kraichnan (1965), who both studied the nonlinear interactions in incompressible MHD: **Momentum**

$$\frac{\partial \boldsymbol{U}}{\partial t} = -\boldsymbol{U}\cdot\nabla\boldsymbol{U} - \frac{1}{\rho_0}\nabla\left(p + \frac{B^2}{8\pi}\right) + \frac{\boldsymbol{B}\cdot\nabla\boldsymbol{B}}{4\pi\rho_0} \tag{I.16}$$

Induction

$$\frac{\partial \boldsymbol{B}}{\partial t} = \nabla\times(\boldsymbol{U}\times\boldsymbol{B}) \tag{I.17}$$

Divergence-free Magnetic Field

$$\nabla\cdot\boldsymbol{B} = 0 \tag{I.18}$$

Divergence-free Flow

$$\nabla\cdot\boldsymbol{U} = 0 \tag{I.19}$$

Beyond adding purely mathematical complexity to this system, the introduction of a magnetic field substantially changes the dynamics. Unlike a mean flow, whose effects can be transformed away, a mean magnetic field, introduces Alfvén waves into the system that causes perturbations to be carried away along the magnetic field. At small enough scales, the large scale field of a magnetized plasma looks like a mean field, and so MHD turbulence can be thought of as a collection of Alfvén wave packets traveling up and down the magnetic field defined by larger scale structures. **This means that there is no single, well-defined mean field that controls the turbulent dynamics at all scales. Rather, it is the structure at slightly larger scales that organizes the the Alfvénic motion and interaction at slightly smaller scales.**

In order to study the nonlinear interactions, it is useful to recast the incompressible MHD equations in terms of the Elsasser variables(Elsasser 1950)

$$\boldsymbol{z}^{\pm} = \boldsymbol{U}_{\perp} \pm \frac{\delta B_{\perp}}{\sqrt{4\pi\rho_0}}. \tag{I.20}$$

This choice of variables yields the symmetric expression

$$\frac{\partial \boldsymbol{z}^{\pm}}{\partial t} \mp (\boldsymbol{v}_A\cdot\nabla)\,\boldsymbol{z}^{\pm} + (\boldsymbol{z}_{\mp}\cdot\nabla)\,\boldsymbol{z}^{\pm} = -\nabla p \tag{I.21}$$

where $\boldsymbol{v}_A = \boldsymbol{B}_0/\sqrt{4\pi\rho_0}$. Physically, $\boldsymbol{z}^+$ represents a nonlinear solution to the MHD equations traveling 'down' $\boldsymbol{B}_0$ at the Alfvén speed, while $\boldsymbol{z}^-$ represents a nonlinear solution to the MHD equations traveling 'up' $\boldsymbol{B}_0$ at the Alfvén speed.

Importantly, the nonlinear term $(\boldsymbol{z}_\mp \cdot \nabla)\,\boldsymbol{z}^\pm$ is non-zero only when both $\boldsymbol{z}^+ \neq 0$ **and** $\boldsymbol{z}^- \neq 0$. Therefore, nonlinear interactions occur only between Alfvén waves traveling in opposite directions along the mean field. As a concrete example, when $\boldsymbol{z}^- = 0$, Eqn. I.21 simplifies to[4]

$$\frac{\partial \boldsymbol{z}^+}{\partial t} - (\boldsymbol{v}_A \cdot \nabla)\,\boldsymbol{z}^+ = 0. \tag{I.22}$$

This describes a wavepacket $\boldsymbol{z}^+$of arbitrary form and amplitude propagating in the $-\boldsymbol{B}_0$ direction. This is an exact nonlinear solution, that holds when all the wave energy is moving in one direction.

When $(\boldsymbol{z}_\mp \cdot \nabla)\,\boldsymbol{z}^\pm \neq 0$, nonlinear interactions arise, allowing for the formation of a turbulent distribution of energy as a function of scale. If the fluctuations are treated as plane waves with a Fourier decomposition, the nonlinear interaction term is $\left(\boldsymbol{z}_\mp \cdot \boldsymbol{k}^\pm\right)\boldsymbol{z}^\pm$. As the Elsasser fluctuation is purely in the plane transverse to $\boldsymbol{B}_0$, we can define a nonlinear frequency

$$\omega^\pm_{\rm nl} \sim \boldsymbol{z}_\mp \cdot k^\pm_\perp \sim k^\pm_\perp v^\mp. \tag{I.23}$$

Thus, if $\boldsymbol{k}^+_\perp = k_\perp \hat{x}$, then it is the $\hat{x}$ component of $\boldsymbol{z}^-$ that leads to nonlinear interactions. Recall that for an Alfven wave with $\boldsymbol{k}^+_\perp = k_\perp \hat{x}$, $\boldsymbol{z}^+ = z^+\hat{y}$.

TLDR: In order for a nonlinear transfer of energy to smaller scales to arise in incompressible MHD, there must be counterpropagating Alfvénic fluctuations, and them must be polarized such that they can shear one another.

I.2.1.1. *Iroshnikov-Kraichnan Spectrum*

Any self-respecting turbulence theory will have not only a description of the basis of the nonlinear interaction, but also a prediction of the spectral index of the inertial range where the nonlinear interactions loss-less-ly transfer energy from scale to scale.

The Iroshnikov-Kraichnan (IK) Spectrum assumes, like hydrodynamic theory, that the transfer of energy to small scales occurs isotropically in wavevector space. The nonlinear interactions occur between Alfvén wave packets of parallel length

$$l_\parallel \sim \frac{1}{k_\parallel} \sim \frac{1}{k} \tag{I.24}$$

The interaction time is given by the Alfvén wave crossing time

$$\tau \sim \frac{1}{k v_A} \sim \frac{1}{\omega}. \tag{I.25}$$

We study the perturbation $\delta v_k/v_k$ occuring in a single collision at wavenumber k

$$\frac{\delta v_k}{v_k} \sim \left(\frac{dv_k}{dt}\tau\right)\frac{1}{v_k} \tag{I.26}$$

Noting that the time rate of change due to nonlinear interactions is

$$\frac{\partial \boldsymbol{z}^\pm}{\partial t} \sim (\boldsymbol{z}_\mp \cdot \nabla)\,\boldsymbol{z}^\pm \sim (k v_k) v_k \tag{I.27}$$

[4]The ∇p term can be shown to vanish by taking the divergence of Eqn. I.21 with $\boldsymbol{z}^- = 0$. Since $\nabla \cdot \boldsymbol{z}^+ = 0$ for incompressible MHD, then $\nabla^2 p = 0$. Thus pressure must be constant everywhere, resulting in Eqn. I.22

we can write

$$\frac{\delta v_k}{v_k} \sim \frac{v_k^2 k}{v_A k}\frac{1}{v_k} \sim \frac{v_k}{v_A}. \tag{I.28}$$

IK theory further assumes that $v_k \ll v_A$ and that these collisions are uncorrelated. This means that the number of random kicks needed to produce an order unity change $\delta v_k \sim v_k$ is

$$N \sim \left(\frac{v_k}{\delta v_k}\right)^2 \sim \left(\frac{v_A}{v_k}\right)^2. \tag{I.29}$$

The cascade time will simply be the interaction time τ times the number of kicks N

$$\tau_{IK} \sim N\tau \sim \left(\frac{v_A}{v_k}\right)^2 \left(\frac{1}{k v_A}\right) \sim \frac{v_A}{k v_k^2} \sim \frac{1}{\omega_k}. \tag{I.30}$$

Assuming a constant energy cascade rate

$$\epsilon = \epsilon_0 = \frac{v_k^2}{\tau_{IK}} = v_k^2 \omega_k = \frac{k v_k^4}{v_A}. \tag{I.31}$$

As a reminder, for the hydrodynamic case, $\epsilon \sim v_k^3 k$. Given that this rate will hold for all scales in the inertial range, we can define

$$\epsilon_0 = \frac{k_0 v_0^4}{v_A} \rightarrow v_k = v_0 \left(\frac{k}{k_0}\right)^{-1/4}. \tag{I.32}$$

The one dimensional energy spectrum of the kinetic energy is thus

$$E_k \sim \frac{v_k^2}{k} \sim v_0^2 k_0^{1/2} \left(\frac{k}{k_0}\right)^{-3/2}. \tag{I.33}$$

This is referred to as the Iroshnikov-Kraichnan Spectrum.

I.2.1.2. *Weakening Turbulence*

If we calculate the number of collisions required to transfer energy from scale k to scale $2k$, N_k, we find

$$N_k \sim \left(\frac{v_A}{v_k}\right)^2 \sim \left(\frac{v_A}{v_0}\right)^2 \left(\frac{k}{k_0}\right)^{1/4} \tag{I.34}$$

or, $N_k \propto k^{1/2}$. In words, the number of collisions required increases with scale, so the nonlinear interactions become weaker at smaller scales.

I.2.2. *Weak MHD Turbulence*

Despite a reasonable enough looking theory, in the decades following IK's original publications, the predicted spectrum did not match those produced by a series of numerical simulations, nor the observations of MHD systems. Additionally, the isotropic transfer of energy to higher $k = \sqrt{k_\parallel^2 + k_\perp^2}$, which is an implicit assumption of IK theory did not agree with numerical simulations that showed a preferential transfer to smaller perpendicular scales $l_\perp$ rather than smaller parallel scales $l_\parallel$.

A refinement to this theory was presented in Sridhar and Goldreich (1994), where the

authors presented a model for weak anisotropic MHD turbulence that accounted for wavevector anisotropy with respect to the orientation of the magnetic field.[5]

Weak Turbulence Theory starts with the proviso that the amplitude of the fluctuations are relatively small, for our case $v_k \ll v_A$. This means that it will take many collisions of Alfvén wave packets before energy is transferred nonlinearly from wavenumber k to wavenumber $2k$ (or from scale l to scale $l/2$). We will treat these small corrections $\delta v_k/v_A$ with perturbation theory.

The dominant interaction between waves will be a three-wave interaction between waves with wavevectors $\boldsymbol{k}_1$, $\boldsymbol{k}_2$, and $\boldsymbol{k}_3$, with frequencies ω_1, ω_2, and ω_3. The conservation of momentum requires that

$$\boldsymbol{k}_1 + \boldsymbol{k}_2 = \boldsymbol{k}_3 \tag{I.35}$$

while the conservation of energy requires[6]

$$\omega_1 + \omega_2 = \omega_3. \tag{I.36}$$

Given that we have stipulated these are Alfvén waves, and assuming $\omega > 0$, with $\omega = |k_\parallel| v_A$, Eqn I.36 becomes

$$|k_{\parallel,1}| + |k_{\parallel,2}| = |k_{\parallel,3}|. \tag{I.37}$$

As we have previously shown, the colliding waves need to be propagating in opposite directions for the nonlinear interaction to be non-zero; we will take $k_{\parallel,1} \geqslant 0$ and $k_{\parallel,2} \leqslant 0$ to satisfy this constraint. The only wave to satisfy the energy conservation constraint and the parallel component of the momentum constraint

$$k_{\parallel,1} + k_{\parallel,2} = k_{\parallel,3} \tag{I.38}$$

is to have $k_{\parallel,2} = 0$, and thus $k_{\parallel,1} = k_{\parallel,3}$. In other words, there is no cascade to higher $k_\parallel$; energy is strickly transferred to higher $k_\perp$ (smaller $l_\perp$) in weak turbulence.[7]

Under these assumptions, let us build a scaling theory for an anisotropic, Weak MHD Turbulent system.

We will continue to assume that the nonlinear interactions occur between oppositely

[5]The original form of this theory was somewhat flawed, but over the next decade of publications and arguments, the errors were corrected and a 'currently accepted' picture has arisen. For those interested in the history of the evolution of this theory, please see the long footnote in Lithwick and Goldreich (2003).

[6]An interpretation of this requirement is to view the wave fields as a collection of wave quanta at different wavenumbers and frequencies, restricting the frequencies to positive values, and assigning a wave quantum at wavevector $\boldsymbol{k}$ and frequency ω_k the momentum $\hbar\boldsymbol{k}$ and energy $\hbar\omega_k$.

[7]There are a number of subtle points about the three-wave (and four-wave) interactions here. The 3-wave interaction conditions were first pointed out in Shebalin et al. (1983). Sridhar and Goldreich (1994) argued that the 3-wave interactions were empty, and weak MHD turbulence must be based on 4-wave interactions. Montgomery and Matthaeus (1995) and Ng and Bhattacharjee (1996) showed that 3-wave interactions were non-zero, which was followed by a response from Goldreich and Sridhar (1997), agreeing that a weak turbulence theory based on 3-wave interactions could be constructed, but that perturbation theory was inapplicable. Galtier et al. (2000) showed that perturbation theory **can** treat the 3-wave interactions, but suggested that the $k_\parallel = 0$ modes may be *problematic*. Lithwick and Goldreich (2003) explained that the $k_\parallel = 0$ modes are fine in perturbation theory as long as correlations times are shorted than cascade times, and that physically, these modes correspond to field line wander. Schekochihin (2020) §4 provides much more detail into this controversy, but for the purposes of this lecture, we will focus on the fact that three-wave interactions are dominant, and will build a weak MHD theory based on such interactions.

directed Alfvén wave packets. Such a packet has transverse scale length of $l_\perp \sim 1/k_\perp$ and parallel scale $l_\parallel \sim 1/k_\parallel$.

The perturbation occuring in a single collision at wavenumber $k_\perp$ is

$$\delta v_k \sim \frac{dv_k}{dt}\tau_c \text{ where } v_k = v_\perp(k_\perp). \tag{I.39}$$

We take the collision time as the Alfvén wave crossing time,

$$\tau_c \sim \frac{l_\parallel}{v_A} \sim \frac{1}{k_\parallel v_A}. \tag{I.40}$$

The nonlinear rate of change is associated with $\dfrac{\partial \boldsymbol{v}}{\partial t} \sim \boldsymbol{v}\cdot\nabla\boldsymbol{v} \sim v_k k_\perp v_k$, where we have taken advantage of the fact thatt $\boldsymbol{v}$ is transverse to the background field for an Alfvén wave. Thus

$$\delta v_k \sim \frac{k_\perp v_k^2}{k_\parallel v_A} \rightarrow \frac{\delta v_k}{v_k} \sim \frac{k_\perp v_k}{k_\parallel v_A}. \tag{I.41}$$

As before, we assume each collision only leads to a small perturbation, and thus many collisions will need to occur to lead to a significant transfer of energy to smaller scales. As with the IK theory, these collisions are uncorrelated, so the number of collisions needed to deform a structure and transfer energy from scale l to scale $l/2$ is

$$N \sim \left(\frac{v_k}{\delta v_k}\right)^2 \sim \left(\frac{k_\parallel v_A}{k_\perp v_k}\right)^2 \gg 1 \tag{I.42}$$

with associated nonlinear energy transfer time

$$\tau_{nl} \sim N\frac{1}{k_\parallel v_A} \sim \frac{k_\parallel v_A}{(k_\perp v_k)^2} \sim \frac{1}{\omega_{nl}}. \tag{I.43}$$

We can thus define the nonlinear transfer frequency as

$$\omega_{nl} \sim \left(\frac{k_\perp v_k}{k_\parallel v_A}\right) k_\perp v_k = \chi k_\perp v_k \tag{I.44}$$

where we introduce the nonlinear parameter

$$\chi \equiv \frac{k_\perp v_k}{k_\parallel v_A}. \tag{I.45}$$

For weak turbulence, $\chi \sim \delta v_k/v_k \ll 1$; physically we can interpret small χ as weak nonlinear interactions.

With a defined nonlinear time, we can define a cascade rate

$$\epsilon \sim v_k^2\omega_{nl} \sim v_k^2\left(\frac{k_\perp v_k}{k_\parallel v_A}\right) k_\perp v_k \sim \left(\frac{k_\perp^2 v_k^4}{k_\parallel v_A}\right) = \epsilon_0 \tag{I.46}$$

and assuming a steady state transfer of energy throughout the inertial range, we have a scaling for the velocity fluctuations

$$v_k = \epsilon_0^{1/4}(k_\parallel v_A)^{1/4} k_\perp^{-1/2} \text{ or } v_k \propto k_\perp^{-1/2}. \tag{I.47}$$

As we have done previously, we can construct a spectrum from the scaling of the velocity fluctuations, but now calculating the energy as a function of $k_\perp$ rather than the

isotropic wavenumber k, $E_{k_\perp} \sim v_k^2/k_\perp$.[8] We can immediately write down

$$E_{k_\perp} \sim \epsilon_0^{1/2} \left(k_\parallel v_A\right)^{1/2} k_\perp^{-2} \text{ or } E_{k_\perp} \propto k_\perp^{-2}. \tag{I.48}$$

This is the predicted weak MHD turbulence spectrum.

I.2.2.1. *Strengthening Turbulence*

Another difference with IK theory is that the number of collisions required to transfer energy from scale to scale decreases with increasing k (decreasing scale-size),

$$N \sim \left(\frac{k_\parallel v_A}{k_\perp v_\perp}\right)^2 \sim \left(\frac{k_\parallel v_A}{k_\perp \epsilon_0^{1/4} (k_\parallel v_A)^{1/4} k_\perp^{-1/2}}\right)^2 \sim \frac{\left(k_\parallel v_A\right)^{3/2}}{\epsilon_0^{1/2}} k_\perp^{-1} \tag{I.49}$$

This means that each collision is stronger.

In terms of the nonlinear parameter χ, we see that the numerator $k_\perp v_k \propto k_\perp^{1/2}$ increases with increasing $k_\perp$ while the demoninator $k_\parallel v_A$ is constant due to the lack of a $k_\parallel$ cascade. Thus, even for weakly turbulent systems with $\chi \ll 1$, with increasing $k_\perp$, $\chi \to 1$, that is the nonlinear interactions get stronger. Once $\chi \sim 1$, $N \to 1$, and all energy cascades in a single collision. Such a system is no longer in a state of weak turbulence, and perturbation theory fails. We have transitioned to **Strong MHD Turbulence**.

In summary, the entire weak MHD cascade only procedes transverse to, rather than along, the background magnetic field. As the strength of the interactions increase, weak MHD turbulence will *always* have a limited range. If the turbulence is driven sufficiently strongly, the range of scales in $k_\perp$ for which weak turbulence theory is valid may be small or non-existent.

I.2.3. *Strong MHD Turbulence*

If we consider a magnetofluid, with energy isotropically injected in at a large scale $k_{\perp,0} = k_{\parallel,0} = k_0$ with relatively weak stiring $v_0 \ll v_A$, some form of weak turbulence will transfer energy anisotropically to smaller perpendicular scales, but *not* to smaller parallel scales. Initially, it will take many Alfvén wave collisions to transfer energy from scale $l_\perp$ to scale $l_\perp/2$, but the strength of the cascade, characterized by the nonlinear parameter $\chi = k_\perp v_k / k_\parallel v_A \propto k_\perp^{1/2}$ will increase as energy is cascaded further into the inertial range. At some perpendicular wavevector $k_\perp > k_{\perp 0}$, the weak turbulence approximation $\chi \ll 1$ will break down. In this limit $\delta v_k / v_k \sim k_\perp v_k / k_\parallel v_A \sim \chi \sim 1$, or physically, *All energy at a scale $k_\perp$ cascades in a single wavepacket collision.* Thus, our assumptions about many uncorrelated kicks leading to a random walk fails, and we will need to produce a new scaling theory.

Additionally, the applicability of pertubation theory ceases. At $\chi \sim 1$, all terms in the perturbative expansion (3-wave, 4-wave, 5-wave... interactions) contribute equally; the 3-wave interaction no longer dominates, and the energy and momentum matching conditions are relaxed. This results in a relaxing of the limitation on the prediction of no parallel cascade. This effect is mathematically captured in Goldreich and Sridhar (1995) in the kinetic equation for the energy transfer by applying a frequency renormalization. Here, we will instead present the scaling of the parallel and perpendicular cascades in terms of the hypothesis of **critical balance**.

I.2.3.1. *Critical Balance*

Goldreich and Sridhar (1995) proposed that in strong turbulence the parallel cascade

[8] For an anisotropic spectra, $E_{k_\perp} = E(k_\perp)$ where $E = \int dk_\perp E(k_\perp) = \int dk_\perp \int_{-\infty}^{\infty} dk_\parallel 2\pi k_\perp E^{(3)}(\boldsymbol{k})$.

occurs in such a manner to maintain $\chi \sim 1$ for increasing $k_\perp$. This concept of critical balance can be interpreted as a balance between the linear and nonlinear terms in the incompressible MHD equations, cast in Elsasser form in Eqn I.21. Effectively, the hypothesis states that, in a strongly turbulent plasma, the parallel cascade occurs in such a manner to maintain $\chi \sim 1$ for larger values of $k_\perp$. Mathematically, this requires a balance between the linear advection term $(\boldsymbol{v}_A \cdot \nabla)\boldsymbol{z}^\pm$ with the nonlinear transfer term $(\boldsymbol{z}^\mp \cdot \nabla)\boldsymbol{z}^\pm$. If we consider the advection of the $\boldsymbol{z}^+$ term, and assume a state of balanced turbulence $\boldsymbol{z}^+ \sim \boldsymbol{z}^-$, we can take $\boldsymbol{z}^+ \sim v_k$. Estimating the linear term, we have

$$\left(\boldsymbol{v}_A \cdot \nabla\right) \boldsymbol{z}^+ \sim v_A k_\parallel z^+ \sim v_A k_\parallel v_k. \tag{I.50}$$

Estimating the nonlinear term, we have

$$\left(\boldsymbol{z}^- \cdot \nabla\right) \boldsymbol{z}^+ \sim z^- k_\parallel z^+ \sim v_k^2 k_\parallel. \tag{I.51}$$

As we have previously expressed, their ratio gives us the nonlinearity parameter χ.

The scale where weak turbulence first reaches $\chi \sim 1$ is very wavevector anisotropic, with $k_\perp \gg k_\parallel$. Recalling our weak turbulence scaling

$$\epsilon \sim \frac{k_\perp^2 v_k^4}{k_\parallel v_A} \sim \epsilon_0 \sim \frac{k_{\perp,0}^2 v_0^4}{k_{\parallel,0} v_A} \rightarrow v_k = v_0 \left(\frac{k_\perp}{k_{\perp,0}}\right)^{-1/2} \tag{I.52}$$

Thus

$$\chi \sim \frac{k_\perp v_k}{k_\parallel v_A} \sim \frac{k_\perp v_0 \left(\frac{k_\perp}{k_{\perp,0}}\right)^{-1/2}}{k_\parallel v_A} \sim \left(\frac{k_\perp}{k_0}\right)^{1/2} \frac{v_0}{v_A} \sim 1. \tag{I.53}$$

Hence,

$$\left(\frac{k_\perp}{k_0}\right)^{1/2} \sim \frac{v_A}{v_0} \rightarrow \frac{k_\perp}{k_\parallel} \sim \left(\frac{v_A}{v_0}\right)^2 \gg 1. \tag{I.54}$$

By the time turbulence transitions from weak to strong, it has become very anisotropic, with much more energy in small perpendicular scale-structures compared to parallel scales.

Let's build ourselves a scaling theory for strongly turbulent system. When $\chi \sim 1$, $\delta v_k / v_k \sim 1$; all the energy is transfered to the next smallest scale in a single collision. Thus, the nonlinear transfer time is

$$\tau_{nl} \sim \frac{1}{k_\parallel v_A} \sim \frac{1}{k_\perp v_k} \sim \frac{1}{\omega_{nl}} \tag{I.55}$$

The energy cascade rate is thus

$$\epsilon \sim \frac{v_k^2}{\tau_{nl}} \sim v_k^2 \omega_{nl} \sim v_k^3 k_\perp = \epsilon_0 \tag{I.56}$$

and therefore $v_k = \epsilon^{1/3} k_\perp^{-1/3}$. We can then immediately write

$$E_{k_\perp} \sim \frac{v_k^2}{k_\perp} \sim \epsilon_0^{2/3} k_\perp^{-5/3} \sim \frac{v_A^2}{k_0} \left(\frac{k_\perp}{k_0}\right)^{-5/3} \tag{I.57}$$

where we have used $\epsilon_0 \sim k_{\perp,0} v_0^3 \sim k_0 v_A^3$ which is the Goldreich-Sridhar, or critically balanced, spectrum. Note that even though the same power law exponent is found as with Kolmogorov, this spectrum scales with $k_\perp$, not the isotropic scale k.

So, if we have left weak turbulence, and its lack of a parallel cascade, behind, how

do we predict that the parallel cascade should proceed? Given that we have based this theory on the equivalence of the linear and nonlinear timescales

$$\omega \sim \omega_{nl} \tag{I.58}$$
$$k_\parallel v_A \sim k_\perp v_k \sim k_\perp \left(\epsilon^{1/3} k_\perp^{-1/3}\right)$$
$$k_\parallel \sim k_0^{1/3} k_\perp^{2/3} \tag{I.59}$$

we see that critical balance predicts a scale-dependent anisotropy

$$\frac{k_\perp}{k_\parallel} \sim \frac{k_\perp}{k_0^{1/3} k_\perp^{2/3}} \sim \left(\frac{k_\perp}{k_0}\right)^{1/3} \tag{I.60}$$

which increases as $k_\perp$ increases. Even for an isotropically driven system, at small scales, critical balance predicts $k_\perp \gg k_\parallel$. This is very important when we consider kinetic turbulence, the continuation of MHD turbulence at scales of order or smaller than the ion Larmor radius, $k_\perp \rho_i \gtrsim 1$.

An important note, this theory does not predict that all energy will be found exactly along the critical balance line in scale space, but rather proposes a distribution of power limited by $\chi \sim 1$.

I.2.3.2. *Beyond Critical Balance*

For those interested, there have been a number of developments beyond and refinements to critical balance, namely incorporating dynamics in the transverse plane with respect to the orientation of the magnetic field, e.g. Boldyrev (2006); Mallet et al. (2015), the effects of imbalanced interactions, e.g. Lithwick et al. (2007), and the impact of intermittent structures on the scale to scale transfer of energy, e.g. Mallet et al. (2017); Loureiro and Boldyrev (2017). This last topic in particular relates the kinds of anisotropic structures generated by turbulence with another fundamental process, that of magnetic reconnection, where the topology of the magnetic field reconfigures, releasing stored magnetic energy into fluid outflows. This process will be the focus of our next lecture.

Recommended Reading:

- For those looking for extensive detail, Schekochihin (2020) presents a 'biased', but lengthy review of the subject, as well as proposes avenues for future research.
- For those looking for observational evidence supporting these predictions of turbulence, Chen (2016a) presents a review of studies of turbulence in the Sun's extended atmosphere, known as the solar wind, made using data from in situ spacecraft observations.

PART II

Kinetic Plasma Processes

Essentially, all models are wrong, but some are useful.
Empirical Model-Building and Response Surfaces
George E. P. Box

II.1. What if collisions aren't strong enough?

We have thus far focused on single particle motion, or on systems in which the physics can be adequately described by a (magneto) fluid. What happens when the collisions that enforce a fluid-like behavior are not strong enough? Must in these cases we revert to tracking the motion of each particle?

Unfortunately, there are simply too many particles to track each individually, and thus we must construct a statistical description for the ensemble of particles. This process of moving from a self consistent description of each and every particle, called the *Klimontovich Equation*, to a more tractable system is through a process called the BBGKY hierarchy (after work by Bogoliubov, Born, Green, Kirkwood, and Yvon) which involves ensemble averaging of the individual particles into a phase-space distribution. Details of this process are discussed in the lecture notes from Prof. Loureiro, as well as in most standard plasma texts; the presentation in Nicholson (1983) is particularly lucid.

For completeness of this document, we introduce the distribution function $f_j(\boldsymbol{x}, \boldsymbol{v}, t)$. Physically, the number of particles of species or component j in the 6D phase-space volume defined by $\Delta\boldsymbol{x}\Delta\boldsymbol{v}$ is represented by $d^3\boldsymbol{x}d^3\boldsymbol{v}f_j(\boldsymbol{x}, \boldsymbol{v}, t)$; in other words, f_j is a number density in a six-dimensional phase space. Where there are no collisions, particles at nearby points move together in a fashion analogous to an incompressible 6D fluid. Taking velocity moments of f_j yields useful quantities, such as the density of species j (the zeroth velocity moment),

$$n_j(\boldsymbol{x}, t) = \int d^3\boldsymbol{v} f_j(\boldsymbol{x}, \boldsymbol{v}, t), \tag{II.1}$$

the fluid velocity (the first velocity moment),

$$\boldsymbol{U}_j(\boldsymbol{x}, t) = \frac{1}{n_j(\boldsymbol{x}, t)} \int d^3\boldsymbol{v}\boldsymbol{v} f_j(\boldsymbol{x}, \boldsymbol{v}, t), \tag{II.2}$$

the kinetic energy density (the second velocity moment)

$$\mathcal{E}_j(\boldsymbol{x}, t) = \int d^3\boldsymbol{v} \frac{m_j v^2}{2} f_j(\boldsymbol{x}, \boldsymbol{v}, t), \tag{II.3}$$

etc. We will investigate the governing equations for f_j, in particular a quintessential kinetic process, Landau damping.

From the BBGKY hierarchy, one can derive a description for the dynamic behavior of the phase-space density (our distribution function f_j). This description takes the form of the Boltzmann (or Vlasov-Landau) equation:

$$\frac{\partial f_j}{\partial t} + \boldsymbol{v} \cdot \nabla f_j + \frac{q_j}{m_j}\left(\boldsymbol{E} + \frac{\boldsymbol{v} \times \boldsymbol{B}}{c}\right) \cdot \frac{\partial f_j}{\partial \boldsymbol{v}} = \left(\frac{\partial f_j}{\partial t}\right)_c \tag{II.4}$$

The Vlasov-Landau equation is closed by the Maxwell equations

$$\nabla \cdot \boldsymbol{E} = 4\pi \sum_j q_j \int d^3\boldsymbol{v} f_j(\boldsymbol{x}, \boldsymbol{v}, t) \tag{II.5}$$

$$\nabla \cdot \boldsymbol{B} = 0 \tag{II.6}$$

$$\nabla \times \boldsymbol{E} = -\frac{1}{c}\frac{\partial \boldsymbol{B}}{\partial t} \tag{II.7}$$

$$\nabla \times \boldsymbol{B} = \frac{1}{c}\frac{\partial \boldsymbol{E}}{\partial t} + \frac{4\pi}{c}\sum_j q_j \int d^3\boldsymbol{v}\boldsymbol{v} f_j(\boldsymbol{x}, \boldsymbol{v}, t) \tag{II.8}$$

The Landau collision operator $\left(\frac{\partial f_j}{\partial t}\right)_c$ on the right hand side of Eqn. II.4 depends on the distribution of component j as well as with all other species or components j'. Without going into gory details, we simply note that the collision operator has the following properties:

$$\int d^3\boldsymbol{v} \left(\frac{\partial f_j}{\partial t}\right)_c = 0 \text{ Conserves individual species particle number} \tag{II.9}$$

$$\sum_j \int d^3\boldsymbol{v} m_j \boldsymbol{v} \left(\frac{\partial f_j}{\partial t}\right)_c = 0 \text{ Conserves total momentum} \tag{II.10}$$

$$\sum_j \int d^3\boldsymbol{v} \frac{m_j v^2}{2} \left(\frac{\partial f_j}{\partial t}\right)_c = 0 \text{ Conserves total energy} \tag{II.11}$$

$$\frac{d}{dt}\left[-\sum_j \int d^3\boldsymbol{x} \int d^3\boldsymbol{v} f_j \ln f_j\right] = -\sum_j \int d^3\boldsymbol{x} \int d^3\boldsymbol{v} \left(\frac{\partial f_j}{\partial t}\right)_c \ln f_j \geqslant 0 \text{ Boltzmann's H theorem} \tag{II.12}$$

$$\left(\frac{\partial f_j}{\partial t}\right)_c \text{ removes small-scale structure in velocity space through diffusion.} \tag{II.13}$$

Expressions similar to the fluid equations presented earlier in this school can be derived by taking moments of Eqn.II.4. The evolution of each moment will depend on the next higher term (n_j on $\boldsymbol{U}_j$, $\boldsymbol{U}_j$ on $\underline{\underline{P}}_j$...), so some choice of how to close your system of moment equations needs to be concocted and justified.

II.2. Landau Damping

So, why do we go to all this trouble to work with f_j when fluid equations seem to provide a decent description of a plasma system? The short answer is that there are some phenomena in a kinetic system that can not be properly captured when the system is reduced to being solely a function of position. The quintessential example of such a phenomenon is Landau damping, the collisionless damping of electrostatic waves via wave-particle resonances. In a fluid, the large rate of collisions prevents any resonant behavior.

II.2.1. *An Intuitive Picture*

To study how energy is transferred between electromagnetic waves and charged particles, we start with a physically intuiative derivation, leaving the traditional, more maths heavy, description to § II.2.2. Versions of this derivation can be found in Chapter 7.6 from Chen (2016b) or Chapter 8.2 from Stix (1992).

We consider how a particle with charge q and mass m moving along the z-axis at speed v_0 behaves in the presence of a changing, small amplitude, electric field. We model the electric field as

$$E(t,z) = E_0 \cos(\omega t - kz)\exp(\epsilon t)\hat{z}. \tag{II.14}$$

The associated frequency and wavelength of the electric wave are ω and k, and the amplitude increases slowly, with $\epsilon \ll 1$. The amplitude of the wave E_0 is assumed to be small enough that the change in the charged particle's trajectory due to the electric field is small over any single wave period. Given these assumptions, how do the position and velocity of the particle vary with time?

Following Newton's 2nd Law, we can immediately write the equations of motion as

$$\frac{dz}{dt} = v_z, \;\; \frac{dv_z}{dt} = \frac{q}{m}E_0 \cos(\omega t - kz)\exp(\epsilon t). \tag{II.15}$$

We will decompose the position and velocity into an equilibrium and perturbation as $z(t) = v_0 t + \delta z(t)$ and $v_z(t) = v_0 + \delta v_z(t)$. From this decomposition, the first-order corrections to the time rate of change of the velocity can be written[9] as

$$\frac{d\delta v_z}{dt} = \frac{q}{m}E\left(t, z(t)\right) \approx \frac{q}{m}E(t, v_0 t) = \frac{q}{m}E_0 \mathcal{R}\left\{\exp\left[\left(i\left(\omega - kv_0\right) + \epsilon\right)t\right]\right\} \tag{II.16}$$

We can use $\int e^{ax}dx = e^{ax}/a$ to write down $\delta v_z(t)$

$$\begin{aligned}
\delta v_z(t) = & \quad \tfrac{q}{m}E_0 \textstyle\int_0^t dt' \mathcal{R}\left\{\exp\left[\left(i\left(\omega - kv_0\right) + \epsilon\right)t'\right]\right\} && \text{(II.17)}\\
= & \quad \tfrac{q}{m}E_0 \mathcal{R}\left\{\tfrac{e^{[i(\omega - kv_0)+\epsilon]t} - 1}{i(\omega - kv_0) + \epsilon}\right\} \\
= & \quad \tfrac{q}{m}E_0 \tfrac{\epsilon e^{\epsilon t}\cos[(\omega - kv_0)t] - \epsilon + (\omega - kv_0)e^{\epsilon t}\sin[(\omega - kv_0)t]}{(\omega - kv_0)^2 + \epsilon^2}.
\end{aligned}$$

Given the perturbed velocity, we can find the perturbed position using $\int (e^{ax} - 1)/a dx = (e^{ax} - ax)/a^2$

$$\begin{aligned}
\delta z(t) = & \quad \textstyle\int_0^t dt' \delta v_z(t') && \text{(II.18)}\\
= & \quad \tfrac{q}{m}E_0 \textstyle\int_0^t dt' \mathcal{R}\left\{\tfrac{e^{[i(\omega - kv_0)+\epsilon]t'} - 1}{i(\omega - kv_0) + \epsilon}\right\} \\
= & \quad \tfrac{q}{m}E_0 \left[\mathcal{R}\left\{\tfrac{e^{[i(\omega - kv_0)+\epsilon]t} - 1}{[i(\omega - kv_0) + \epsilon]^2}\right\} - \tfrac{\epsilon t}{(\omega - kv_0)^2 - \epsilon^2}\right] \\
= & \quad \tfrac{q}{m}E_0 \left\{\tfrac{[\epsilon^2 - (\omega - kv_0)^2][e^{\epsilon t}\cos[(\omega - kv_0)t] - 1] + 2\epsilon(\omega - kv_0)e^{\epsilon t}\sin[(\omega - kv_0)t]}{[(\omega - kv_0)^2 + \epsilon^2]^2}\right. && \text{(II.19)}\\
& \qquad \left. - \tfrac{\epsilon t}{(\omega - kv_0)^2 + \epsilon^2}\right\}. && \text{(II.20)}
\end{aligned}$$

The perturbation to the electric field is

$$\delta E(t,z) = E(t,z) - E(t, v_0 t) = \delta z(t)\frac{\partial E(t, v_0 t)}{\partial z} = \delta z(t) k \sin\left[\left(\omega - kv_0\right)t\right] E_0 \exp[\epsilon t]. \tag{II.21}$$

Given this field, and the position and velocity of the charged particle, what is the average power transfered between the wave to the particle?

[9] Recall Euler's Identity $\exp[i\theta] = \cos\theta + i\sin\theta$

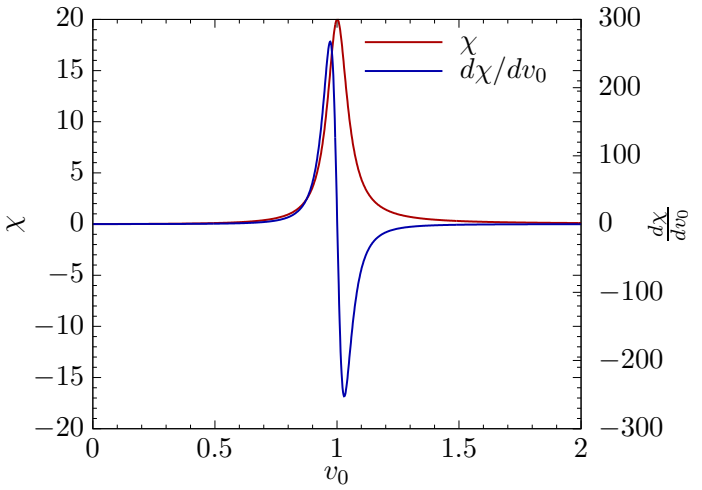

FIGURE 1. The resonant function χ, Eqn. II.25 and its velocity derivative for $\omega = k = 1$ and $\epsilon = 0.05$.

$$P(v_0) = q\,\langle E(t, z(t))v_z(t)\rangle \approx q\,\langle [E(t, v_0t) + \delta E(t, z)]\,[v_0 + \delta v_z(t)]\rangle \tag{II.22}$$

If we average over a time longer than a waveperiod ω^{-1} but shorter than the growth of the wave amplitude ϵ^{-1}, we can simplify this expression.

$$\begin{aligned} P(v_0) \approx \quad & q\,\langle [E(t, v_0t) + \delta E(t, z)]\,[v_0 + \delta v_z(t)]\rangle \\ = \; & q\,\langle v_0E(t, v_0t) + \delta v_z(t)E(t, v_0t) + v_0\delta E(t, z)\rangle + \mathcal{O}[2] \end{aligned} \tag{II.23}$$

The $\mathcal{O}[0]$ term vanishes after averaging. For the $\mathcal{O}[1]$ terms, only the $\cos^2$ term in $\delta v_z(t)E(t, v_0t)$ and the $\sin^2$ term in $v_0\delta E(t, z)$ survive averaging, leaving the somewhat managable expression

$$\begin{aligned} P(v_0) &= qE_0e^{\epsilon t}\left\langle \tfrac{qE_0}{m}\tfrac{\epsilon e^{\epsilon t}\cos^2[(\omega-kv_0)t]}{(\omega-kv_0)^2+\epsilon^2} + \tfrac{qE_0}{m}\tfrac{2\epsilon kv_0e^{\epsilon t}(\omega-kv_0)\sin^2[(\omega-kv_0)t]}{[(\omega-kv_0)^2+\epsilon^2]^2}\right\rangle \\ &= \tfrac{q^2E_0^2}{2m}e^{2\epsilon t}\left[\tfrac{\epsilon}{(\omega-kv_0)^2+\epsilon^2} + \tfrac{2\epsilon kv_0(\omega-kv_0)}{[(\omega-kv_0)^2+\epsilon^2]^2}\right] \\ &= \tfrac{q^2E_0^2}{2m}e^{2\epsilon t}\tfrac{d}{dv_0}\left[\tfrac{\epsilon v_0}{(\omega-kv_0)^2+\epsilon^2}\right] \end{aligned} \tag{II.24}$$

Plotting in Fig. 1 the function inside the velocity derivative,

$$\chi = \frac{\epsilon v_0}{(\omega - kv_0)^2 + \epsilon^2} \tag{II.25}$$

we see that if the initial velocity v_0 is less than the resonant velocity ω/k—the particle lags behind the wave phase velocity— than the velocity derivative is positive and thus the particle gains energy. If the particle is slightly faster than than the wave phase speed, the velocity derivative is negative, and the particle loses energy to the wave.

We know that this particle isn't the only ion or electron moving through this system, so let's consider this single particle as part of an entire distribution of particles $f(v_z)$, and investigate the how the wave affects, and is effected by, the collection of particles.

The total power the distribution will absorb or emit will simply be the integral of

$P(v_z)$ times the density of particles $f(v_z)$ integrated over all possible velocities,

$$\begin{aligned} P &= \int dv_z f(v_z) P(v_z) = \tfrac{q^2 E_0^2}{2m} e^{2\epsilon t} \int dv_z f(v_z) \tfrac{d\chi}{dv_z} \\ &= -\tfrac{q^2 E_0^2}{2m} e^{2\epsilon t} \int dv_z f'(v_z) \chi \end{aligned} \tag{II.26}$$

Taking the limit where $\epsilon \to 0$, and applying *Plemelj's Formula* allows us to write χ as a Dirac delta function

$$\lim_{\epsilon \to +0} \chi(v_z) = \frac{\pi\omega}{k^2} \delta(v_z - \omega/k) \tag{II.27}$$

enabling the swift solution of our integral,

$$P = -\frac{q^2 E_0^2}{2m} \frac{\pi\omega}{k^2} f'\left(\frac{\omega}{k}\right). \tag{II.28}$$

So long as $\omega f'\left(\frac{\omega}{k}\right) < 0$, the wave will damp, and energy will be transferred to the particle distribution. We will consider the case where $\omega f'\left(\frac{\omega}{k}\right) > 0$ in the discussion of kinetic instabilities.

What is physically happening here? For some electrostatic wave with wavenumber $k = 2\pi/\lambda$ and real frequency ω_r. For a velocity distribution that has a negative velocity gradient $\partial f_j / \partial v < 0$ at the resonant velocity $v_\mathrm{res} = \omega_\mathrm{r}/k$, there are more particles slightly slower that ω_r/k than there are those slightly faster than ω_r/k. The slower particles are accelerated by the electric field seen in their reference frame, while the faster particles are decelerated. As there are more slow particles than fast, the wave loses energy, damping away and the distribution of particles gains that energy. This is Landau damping. This process of energy transfer to and from particles depending on their velocity couples with shearing in phase-space to form velocity-space structure in the distribution function due; see Fig. 3. Eventually, the structure is fine enough that collisions begin to act, smoothing out wiggles in $f_j(\boldsymbol{v})$ and increasing entropy, leading to the heating of the charged particles.

II.2.2. *The More Detailed Calculation*

The traditional calculation that you will see in many texts, and the one first derived in Landau (1946), is for plasma oscillations. Here, we will consider the case of ion-acoustic waves, under the simplifying assumptions of low frequencies and quasi-neutrality. The details of this derivation won't be discussed in lecture, but are included for pedagogical completeness.

We start with the electrostatic Vlasov Equation (with no collisions)

$$\frac{\partial f_j}{\partial t} + \boldsymbol{v} \cdot \nabla f_j - \frac{q_j}{m_j} \boldsymbol{E} \cdot \frac{\partial f_j}{\partial \boldsymbol{v}} = 0 \tag{II.29}$$

and linearize, assuming the distribution function can be decomposed into an equilibrium and small perturbation $f_j = F_j(\boldsymbol{v}) + \epsilon \delta f_j(\boldsymbol{x}, \boldsymbol{v}, t)$ and the electric field is purely composed of small-amplitude fluctuations with no mean value $\boldsymbol{E} = \epsilon \delta \boldsymbol{E}(\boldsymbol{x}, t)$. Inserting these expressions into Eqn. II.29 and retaining terms of $\mathcal{O}(\epsilon^1)$ produces

$$\left(\frac{\partial}{\partial t} + \boldsymbol{v} \cdot \nabla\right) \delta f_j(\boldsymbol{x}, \boldsymbol{v}, t) + \frac{q_j}{m_j} \delta \boldsymbol{E} \cdot \frac{\partial F_j(\boldsymbol{v})}{\partial \boldsymbol{v}} = 0. \tag{II.30}$$

To determine the evolution of the electric field perturbations, we will use quasi-neutrality

$$\sum_j q_j \delta n_j = \sum_j q_j \int d^3\boldsymbol{v} \delta f_j(\boldsymbol{x}, \boldsymbol{v}, t) = 0. \tag{II.31}$$

Instead of taking the well-trod path of Fourier transforming in both space and time, which was done in Vlasov (1945), the solution must be solved as an initial value problem, Fourier transforming in space while performing a Laplace transform[10] in time. These transforms are defined as [11]

$$f(\boldsymbol{k}) = \int \frac{d^3\boldsymbol{x}}{(2\pi)^3} e^{-i\boldsymbol{k}\cdot\boldsymbol{x}} f(\boldsymbol{x}) \tag{II.32}$$

$$f(\omega) = \int_0^\infty dt e^{i\omega t} f(t). \tag{II.33}$$

Under a Fourier transform in space and Laplace transform in time, Eqn. II.30 becomes

$$(-i\omega + i\boldsymbol{k}\cdot\boldsymbol{v})\,\delta f_j(\boldsymbol{k},\boldsymbol{v},\omega) - \delta f_j(\boldsymbol{k},\boldsymbol{v},t=0) + \frac{q_j}{m_j}\delta\boldsymbol{E}(\boldsymbol{k},\omega)\cdot\frac{\partial F_j(\boldsymbol{v})}{\partial\boldsymbol{v}} = 0 \tag{II.34}$$

where we have exploited the nature of the time derivative under a Laplace transform $f_j'(\omega) = -i\omega f_j(\omega) - f_j(t=0)$ where the last term is the initial value of f_j at time $t = 0$.

This can be rearranged to yield an expression for the transformed distribution function

$$\delta f_j(\boldsymbol{k},\boldsymbol{v},\omega) = \frac{\delta f_j(\boldsymbol{k},\boldsymbol{v},t=0)}{-i\,(\omega - \boldsymbol{k}\cdot\boldsymbol{v})} - \frac{q_j}{m_j}\left[\frac{\delta\boldsymbol{E}(\boldsymbol{k},\omega)\cdot\frac{\partial F_j(\boldsymbol{v})}{\partial\boldsymbol{v}}}{-i\,(\omega - \boldsymbol{k}\cdot\boldsymbol{v})}\right]. \tag{II.35}$$

We next need to eliminate δE. This can be done by using Eqn. II.31 and substituting in $\delta f_j(\boldsymbol{k},\boldsymbol{v},\omega)$

$$\sum_j q_j \int d^3\boldsymbol{v}\frac{\delta f_j(\boldsymbol{k},\boldsymbol{v},t=0)}{-i\,(\omega - \boldsymbol{k}\cdot\boldsymbol{v})} - \sum_j \frac{q_j^2}{m_j}\delta\boldsymbol{E}(\boldsymbol{k},\omega)\cdot\int d^3\boldsymbol{v}\frac{\frac{\partial F_j(\boldsymbol{v})}{\partial\boldsymbol{v}}}{-i\,(\omega - \boldsymbol{k}\cdot\boldsymbol{v})} = 0. \tag{II.36}$$

Assigning the direction of $\delta\boldsymbol{E}$ as $\parallel$, we can write

$$\delta E_\parallel(\boldsymbol{k},\omega) = \frac{\sum_j q_j \int d^3\boldsymbol{v}\frac{\delta f_j(\boldsymbol{k},\boldsymbol{v},t=0)}{-i(\omega-\boldsymbol{k}\cdot\boldsymbol{v})}}{\sum_j \frac{q_j^2}{m_j}\int \frac{\partial F_j(\boldsymbol{v})}{\partial v_\parallel}\frac{d^3\boldsymbol{v}}{-i(\omega-\boldsymbol{k}\cdot\boldsymbol{v})}}. \tag{II.37}$$

In the electrostatic case, $\delta\boldsymbol{E}(\boldsymbol{k},\omega) = -i\boldsymbol{k}\phi(\boldsymbol{k},\omega)$, allowing us to write

$$\phi(\boldsymbol{k},\omega) = \frac{4\pi}{k^2}\frac{1}{D(\boldsymbol{k},\omega)}\sum_j q_j \int d^3\boldsymbol{v}\frac{\delta f_j(\boldsymbol{k},\boldsymbol{v},t=0)}{-i\,(\omega - \boldsymbol{k}\cdot\boldsymbol{v})} \tag{II.38}$$

where the dielectric function is defined as

$$D(\boldsymbol{k},\omega) = \frac{4\pi}{k^2}\sum_j \frac{q_j^2}{m_j}\int d^3\boldsymbol{v}\frac{\boldsymbol{k}\cdot\partial F_j/\partial\boldsymbol{v}}{(\omega - \boldsymbol{k}\cdot\boldsymbol{v})}. \tag{II.39}$$

Physically, values of $\omega(\boldsymbol{k})$ where $D(\boldsymbol{k},\omega) = 0$ represent normal mode solutions for the linear response of the plasma.

Our solution for δE can be in turn substituted back into Eqn. II.35 to yield an

[10] Some texts will use $p = -i\omega$ instead of ω for the Laplace transform. Take care in moving between sources.

[11] See the introductory section of Landau (1946) for critiques of the Fourier transform in both time and space and the necessity of solving this as an intitial value problem.

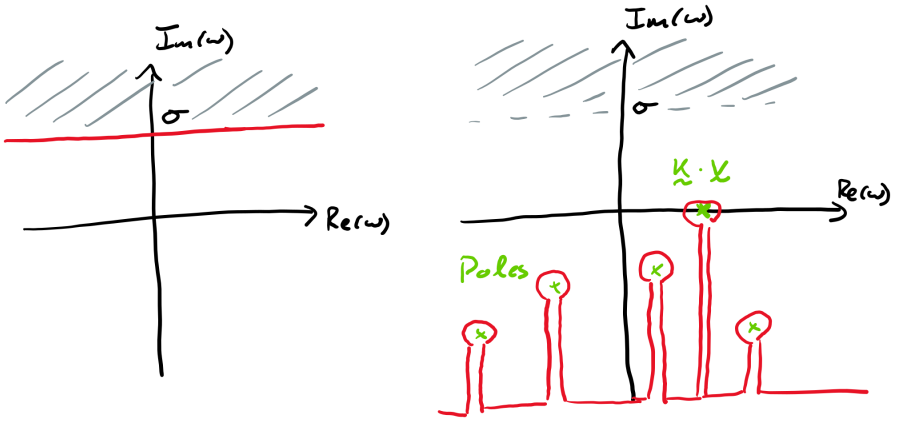

FIGURE 2. The contour used for the inverse Laplace transform (Eqn. II.41, left) as well as the deformed contour used in the specific evaluations of Eqns. II.42 and II.43.

expression for δf_j:

$$\delta f_j(\boldsymbol{k},\boldsymbol{v},\omega) = \frac{\delta f_j(\boldsymbol{k},\boldsymbol{v},t=0)}{-i\left(\omega-\boldsymbol{k}\cdot\boldsymbol{v}\right)} - \frac{q_s}{m_s}\frac{\partial F_j(\boldsymbol{v})}{\partial v_\parallel}\frac{1}{-i\left(\omega-\boldsymbol{k}\cdot\boldsymbol{v}\right)}\left[\frac{\sum_{s'} q_{s'}\int d^3\boldsymbol{v}'\frac{\delta f_{s'}(\boldsymbol{k},\boldsymbol{v}',t=0)}{-i(\omega-\boldsymbol{k}\cdot\boldsymbol{v}')}}{\sum_{s'}\frac{q_{s'}^2}{m_{s'}}\int\frac{\partial F_{s'}(\boldsymbol{v}')}{\partial v_\parallel'}\frac{d^3\boldsymbol{v}'}{-i(\omega-\boldsymbol{k}\cdot\boldsymbol{v}')}}\right] \tag{II.40}$$

In order to extract $\delta f_j(\boldsymbol{x},\boldsymbol{v},t)$ from the above, an inverse-Laplace transform will need to be performed on Eqn. II.40 of the form

$$f(t) = \int_L \frac{d\omega}{2\pi} e^{-i\omega t} f(\omega) \tag{II.41}$$

where L is the Laplace contour, a straight line in complex frequency space parallel to the real ω axis (see the left panel of Fig. 2). The contour intersects the imaginary ω axis at value σ; as long as there exists $\sigma \in \mathcal{R} \ni |f(t)| < e^{\sigma t}$ as $t \to \infty$, the Laplace transform integral exists $\forall\omega \ni \mathcal{I}(\omega) \geqslant \sigma$. (see your favorite book on complex analysis for more details (e.g. Brown and Churchill 2004; Arfken et al. 2013)).

The inverse transforms can be written as

$$\phi(\boldsymbol{k},t) = \int_L \frac{d\omega}{2\pi} e^{-i\omega t}\frac{4\pi}{k^2}\frac{1}{D(\boldsymbol{k},\omega)}\sum_j q_j \int d^3\boldsymbol{v}\frac{\delta f_j(\boldsymbol{k},\boldsymbol{v},t=0)}{-i\left(\omega-\boldsymbol{k}\cdot\boldsymbol{v}\right)} \tag{II.42}$$

and

$$\begin{aligned}\delta f_j(\boldsymbol{k},\boldsymbol{v},t) = &\int_L \frac{d\omega}{2\pi} e^{-i\omega t}\frac{\delta f_j(\boldsymbol{k},\boldsymbol{v},t=0)}{-i\left(\omega-\boldsymbol{k}\cdot\boldsymbol{v}\right)} \\ &- \int_L \frac{d\omega}{2\pi} e^{-i\omega t}\left\{\left[\frac{\sum_{s'}\frac{q_j q_{s'}}{m_j}\frac{\partial F_j(\boldsymbol{v})/\partial v_\parallel}{-i(\omega-\boldsymbol{k}\cdot\boldsymbol{v})}\int d^3\boldsymbol{v}'\frac{\delta f_j(\boldsymbol{k},\boldsymbol{v}',t=0)}{(\omega-\boldsymbol{k}\cdot\boldsymbol{v}')}}{\sum_{s'}\frac{q_{s'}^2}{m_j}\int\frac{\partial F_j(\boldsymbol{v}')}{\partial v_\parallel'}\frac{d^3\boldsymbol{v}'}{(\omega-\boldsymbol{k}\cdot\boldsymbol{v}')}}\right]\right\}\end{aligned} \tag{II.43}$$

To perform this integral, the Laplace contour L must be shifted to $-\infty$. However, the contour can not cross any of the poles of $\delta f_j(\boldsymbol{k},\boldsymbol{v},t)$ (e.g. $\omega = \boldsymbol{k}\cdot\boldsymbol{v}$ or at a normal mode frequency of the system). To do this, one performs an **analytic continuation** of the contour, deforming it around all of the poles of the system. This deformation is illustrated in the right hand panel of Fig. 2. Again, more details can be found in Brown and Churchill (2004) or a plasma textbook of your choosing.

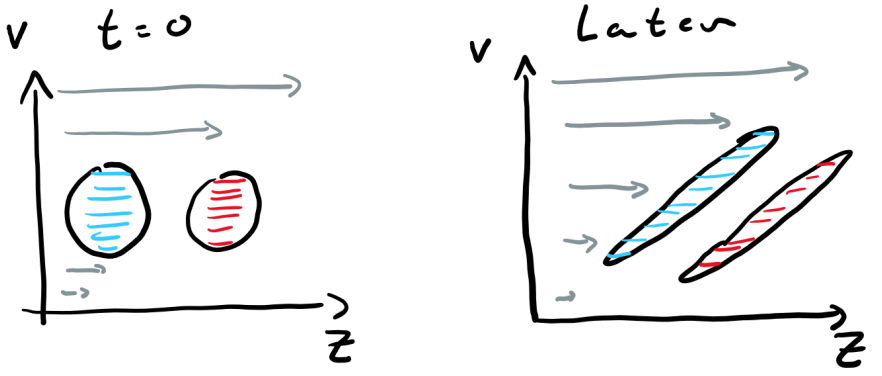

FIGURE 3. Shear of phase-space structure with advancing time leads to the formation of small-scale structure.

This analytic continuation allows us to write the transformed quantities in the form

$$\sum_j \frac{c_j}{-i\left(\omega-\omega_j\right)} + A(\omega) \tag{II.44}$$

where ω_j are the poles of the quantity in question.

One can perform the integrals in Eqns. II.42 and II.43 through the application of Cauchy's residue theorem (complex analysis arises with suprising frequency in kinetic plasma physics...). In performing these integrals, we find that

$$\begin{aligned}\phi(\boldsymbol{k},t) &= \int_L \frac{d\omega}{2\pi} e^{-i\omega t}\left[\sum_j \frac{c_j}{-i\left(\omega-\omega_j\right)} + A(\omega)\right] \\ &= \sum_j c_j \exp\left(-i\omega_j t\right)\end{aligned} \tag{II.45}$$

where the poles here are the zeros of $D(\boldsymbol{k},\omega)$ (representing the normal mode solutions) and those of the initial condition. The physical interpretation of the above is that $\phi(\boldsymbol{k},t)$ is the sum of a number of damped modes.

The behavior of the distribution function is slightly different. Carrying out the inverse-Laplace transform yields

$$\begin{aligned}\delta f_j(\boldsymbol{k},\boldsymbol{v},t) = &\left[\delta f_j(\boldsymbol{k},\boldsymbol{v},t=0) - \frac{q_j}{m_j} i\boldsymbol{k}\cdot\frac{\partial F_j}{\partial \boldsymbol{v}} \sum_j \frac{c_j}{-i\omega_j + i\boldsymbol{k}\cdot\boldsymbol{v}}\right]\exp\left(-i\boldsymbol{k}\cdot\boldsymbol{v}t\right) \\ &+ \frac{q_j}{m_j} i\boldsymbol{k}\cdot\frac{\partial F_j}{\partial \boldsymbol{v}} \sum_j \frac{c_j \exp\left(-i\omega_j t\right)}{-i\omega_j + i\boldsymbol{k}\cdot\boldsymbol{v}}.\end{aligned} \tag{II.46}$$

What does this mean? The time-dependent behavior of the distribution function is a combination of decaying eigenmode solutions and a *ballistic response* (the $\exp\left(-i\boldsymbol{k}\cdot\boldsymbol{v}t\right)$ terms) which oscillate without decaying.

So, we have a potential that decays with time, and a particle distribution that has decaying and non-decaying terms; these terms act in concert to conserve the free energy of the system as the potential decays by transferring energy to the distribution. **This transfer of energy from electrostatic potential fluctuations to the perturbed distribution is Landau damping**. The results of the transfer is the formation of

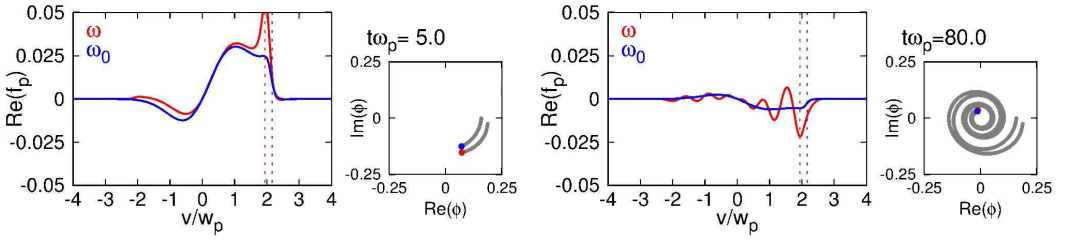

FIGURE 4. Time evolution of the Landau damping of a perturbed velocity distribution and the associated electrostatic potential. An Artificial removal of the ballistic term (blue) removes the formation of small scale velocity space structure see in the physical system (red).

small scale structure in the distribution as a function of velocity scale. This shearing is illustrated at two times (early and late) for a simple system in Fig.4. Eventually the small scale structure gets small enough, and even an minuscule level of collisionality will act to smooth out the distribution.

II.2.3. *Some Actual Calculations*

After having patiently sat through the above mathematical manipulations, let's turn to some more quantitative calculations with more practical applications. For instance, how quickly does Landau damping actually damp a wave? To answer that, we will have to start making some assumptions, such as that the background distribution is a Maxwellian

$$F_j = \frac{n_{0j}}{\pi^{3/2} w_j^3} \exp\left(\frac{-v^2}{w_j^2}\right) \tag{II.47}$$

where the thermal velocity is defined $w_j \equiv \sqrt{2T_{0s}/m_j}$. Let's solve $D(\omega, \boldsymbol{k}) = 0$ (see Eqn. II.39).

$$\begin{aligned} D(\omega,\boldsymbol{k}) &= \sum_j \frac{4\pi}{k^2}\frac{q_j^2}{m_j}\int d^3\boldsymbol{v}\frac{-2\boldsymbol{k}\cdot\boldsymbol{v}}{w_j^2}\frac{F_j}{\omega-\boldsymbol{k}\cdot\boldsymbol{v}} \\ &= \sum_j \frac{4\pi q_j^2 n_{0j}}{k^2 T_{0s}}\int_0^\infty \frac{dv_\perp^2}{w_j^2}\exp\left(-\frac{v_\perp^2}{w_j^2}\right)\int_0^\infty \frac{dv_\parallel}{\sqrt{\pi}w_j}\frac{\exp\left(-\frac{v_\parallel^2}{w_j^2}\right)v_\parallel}{v_\parallel-\omega/k_\parallel} \\ &= \sum_j \frac{4\pi q_j^2 n_{0j}}{k^2 T_{0s}}\left[1+\xi_j Z(\xi_j)\right] = 0. \end{aligned} \tag{II.48}$$

The plasma dispersion function

$$Z(\xi) = \pi^{-1/2}\int_{-\infty}^{\infty}\frac{dt\exp\left(-t^2\right)}{t-\xi} \tag{II.49}$$

with argument $\xi_j = \omega/k_\parallel w_j$ is a frequently employed function in plasma physics. Many of its features and limits are discussed in Fried and Conte (1961), and the most useful ones can be found in the NRL Plasma Formulary. One useful feature of Z is that for $\xi_j \ll 1$, $Z(\xi_j) \approx i\sqrt{\pi}$. Also, we can use the large difference in ion and electron masses ($m_p \approx 1836 m_e$) to write $\xi_e \sim \xi_i\sqrt{m_e/m_i} \ll \xi_i$, effectivitly eliminating $\xi_e Z(\xi_e) \ll 1$ from Eqn. II.49, which can be simply expressed as

$$\xi_i Z(\xi_i) = -(1+\tau) \tag{II.50}$$

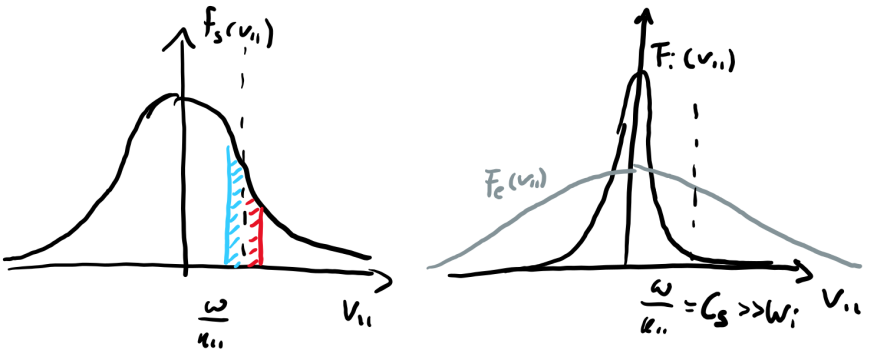

FIGURE 5. Comparison of ion and electron velocity distributions.

where $\tau \equiv (q_e/q_i)(T_{0i}/T_{0s})$. This is the ion-acoustic wave dispersion relation. These waves experience Landau damping. Let's characterize that damping.

We consider the case where $|\xi_i| \gg 1$ (or $\omega \gg k_{\parallel} w_i$) and for weak damping $(\gamma/\omega_{\rm r}) \ll 1$, where γ and $\omega_{\rm r}$ represent the damping rate and real frequency of the normal mode solution. In this limit,

$$\xi_i Z(\xi_i) \approx i\sqrt{\pi}\xi_i e^{-\xi_i^2} - 1 - \frac{1}{2\xi_i^2} + \mathcal{O}(\frac{1}{\xi_i^4}). \tag{II.51}$$

Using this limit, Eqn.II.50 becomes

$$i\sqrt{\pi}\xi_i e^{-\xi_i^2} - \frac{1}{2\xi_i^2} = -\tau. \tag{II.52}$$

This can be separated into real and imaginary components, which after some manipulation yields a real frequency

$$\omega = |k_{\parallel}|\sqrt{\frac{T_e}{m_i}} = |k_{\parallel}|c_s \tag{II.53}$$

and a damping rate

$$\gamma = -|k_{\parallel}|w_i\sqrt{\pi}e^{-\xi_i^2}\xi_i^4. \tag{II.54}$$

To ensure a posteriori that $(\gamma/\omega) << 1$, we take calculate the ratio

$$\frac{\gamma}{\omega} = -\sqrt{\pi}\left(\frac{T_e}{2T_i}\right)^{3/2}\exp\left(-\frac{T_e}{2T_i}\right), \tag{II.55}$$

and find that our solution is consistent with our assumptions as long as $T_e \gg T_i$. This is the Landau damping rate of an ion-acoustic wave.

So, what is happening here? There are some particles that have speeds $v_{\parallel} \sim \omega/k_{\parallel}$. For the case of Landau damping, left panel of Fig. 5, there are more particles slightly slower than the resonant velocity than slightly faster (look ahead to the next lecture for the case of resonant instabilities). The lagging particles will see a stationary electric field in their reference frame and be accelerated; the leading particle will also see a stationary field, but be decelerated. As there are more particles gaining energy than losing energy, the wave damps, eventually flattening the distribution near the resonant velocity. A quantitative treatment of such flattening must be tackled with quasilinear theory, a topic beyond the scope of this lecture.

The more particles near the resonant velocity, the stronger the damping. This is why

Landau damping is relatively weak in the case of $T_i/T_e \ll 1$ (right panel of Fig. 5); for a cold proton distribution with $c_s \ll w_i$, there are few particles that can act to damp the wave. For a hotter distribution of protons, with $c_s \sim w_i$, the damping can be much, much stronger.

Takeaway Points:

- When collisions are insufficiently strong to enforce fluid-like behavior, phenomena associated with the velocity distribution of particles arise.
- The cannonical collisionless phenomenon is Landau damping, a transfer of energy from electrostatic waves to the particle distribution via a wave-particle resonance. This transfer leads to the formation of small scale structure in the velocity distribution.
- The strength of the damping is dependent on the number of particles near the resonant velocity, and the slope of the velocity distribution at that same point.
- A refresher on complex analysis is useful for working through plasma kinetic theory.

Medicine makes people ill,
theology makes them sinful, and
mathematics makes them sad.

Martin Luther

II.3. Kinetic Instabilities

While the Vlasov equation neglects collisions that act to move the plasma system towards a lower energy state, other mechanisms are retained that can perform that role in moving the system toward thermodynamic equilibrium. These mechanisms are called instabilities. Instabilities cause an initially small perturbation to grow, rather than damp, with time. In this lecture we will focus on the how departures from thermodynamic equilibrium in the velocity distribution of the constituent species, $f_j(\boldsymbol{x}, \boldsymbol{v}, t)$, rather than cases where there is free energy available to the system purely in configuration space (e.g. the Kelvin-Helmholtz instability).

II.3.1. *General Stability Considerations*

We start somewhat more abstractly, asking if there are conditions under which stability can be guaranteed.

We return to the ground work laid out in the previous lecture, where we wrote that solutions that satisfy

$$D(\omega, \boldsymbol{k}) = 1 - \sum_s \frac{4\pi}{k^2} \frac{q_s^2}{m_s} \int d^3\boldsymbol{v} \frac{\boldsymbol{k} \cdot \partial F_s / \partial \boldsymbol{v}}{(\omega - \boldsymbol{k} \cdot \boldsymbol{v})} = 0 \tag{II.56}$$

are the normal mode solutions for the electrostatic Vlasov-Poisson system.[12]

We will consider the case of a monotonically decreasing function F_s, and assume that there exists an unstable solution, that is that $\gamma = \mathcal{I}(\omega) > 0$. We define $\omega_r = \mathcal{R}(\omega)$.

One can separate $D(\omega, \boldsymbol{k}) = 0$ into its real and imaginary components, which must separately satisfy the equality:

$$D_r = 1 - \frac{4\pi}{k^2} \sum_s \frac{q_s^2}{m_s} \int_{-\infty}^{\infty} dv \frac{(v - \omega/k)\partial F_s/\partial v}{(v - \omega_r/|k|)^2 + \gamma^2/k^2} = 0 \tag{II.57}$$

$$D_i = \sum_s \int_{-\infty}^{\infty} dv \frac{\gamma/k \partial F_s/\partial v}{(v - \omega_r/|k|)^2 + \gamma^2/k^2} = 0 \tag{II.58}$$

Importantly, for a monotonically decreasing function, $v\partial F/\partial v \leqslant 0$ for all v, and therefore the real component integral in Eqn II.57 cannot be satisfied for all $\gamma > 0$. This statement is know as Gardner's Theorem: If a distribution decreases monotonically away from its maximum, the distribution is stable. Importantly, this does not depend on the frame of reference selected. As long as there exists a frame for which F is monotonically decreasing, F is stable.

Instead of using a proof by contradiction, we can also cast this theorem in terms of thermodynamics. Assuming conservation of energy, and a conservation of volume in (6D) phase space, which is guaranteed by the Vlasov equation, we consider some initial distribution $F(x, u^2, 0)$ that has regions of phase space with different densities. Stability is determined by asking what state, accessible by the initial state has the least kinetic

[12] Eqn II.39 dropped the factor of 1 due to the low-frequency approximation assumed in the enforcement of quasineutrality.

energy, as defined by

$$\int dxdu \frac{mu^2}{2} F(x, u^2). \tag{II.59}$$

Because of the weighing by u^2, the lowest energy value will be achieved when the greatest phase-space densities are near $u^2 = 0$; in terms of a fluid analogy, the 'heaviest' layers at the 'bottom' represent the lowest energy state. If the distribution is already arranged in such a fashion, as is the case for a monotonically decreasing function, then the only kinetic energy available to be transferred to the fields is the energy in any initial perturbation. These perturbations can not grow in time, and thus the distribution is stable.

II.3.2. *Two-Stream Instability*

So, a single monotonically decreasing function can't be unstable. The next obvious case to try is the sum of two distributions. They can't have overlapping maxima, otherwise they would add up to a single monotonically decreasing function. Such a system of two separate populations is typically referred to as a two-stream system when the populations are of similar density, or a bump-on-tail (or beam and core) distribution when one population is much smaller.

Let's start with the two-stream case, with a ion beam moving relative to the electrons. For simplicity, treat the distributions as delta functions:

$$F_i = \delta\left(v - \frac{\boldsymbol{k}\cdot\boldsymbol{V}_0}{|k|}\right) \tag{II.60}$$

$$F_e = \delta\left(v\right). \tag{II.61}$$

This makes the integrals in D trivial, resulting in

$$1 = \frac{\omega_{pe}^2}{\omega^2} + \frac{\omega_{pi}^2}{\left(\boldsymbol{k}\cdot\boldsymbol{V}_0 - \omega\right)^2} \tag{II.62}$$

with the plasma frequency defined as $\omega_{ps}^2 = 4\pi n_s q_s^2/m_s$.

Plotting the right hand side of Eqn II.62, we see real roots given by the intersection of the functional curve with 1. When the minimum of the curve is above 1, we have two real and two imaginary solutions, one of the later is the unstable mode. One can determine that this minimum arises at

$$\omega_A = \boldsymbol{k}\cdot\boldsymbol{V}_0\left[\frac{\left(\omega_{pe}/\omega_{pi}\right)^2}{\left(\omega_{pe}/\omega_{pi}\right)^{2/3}+1}\right] \tag{II.63}$$

and that the condition for the right hand side of Eqn II.62 to be greater than 1 at ω_A is

$$|\boldsymbol{k}\cdot\boldsymbol{V}_0| < \omega_{pe}\left[1+\left(\frac{\omega_{pi}}{\omega_{pe}}\right)^{2/3}\right]^{3/2}. \tag{II.64}$$

We could have equally well looked at the case of two electron beams, or two ion beams, as no sign of the charge of the species was included in the analysis. Importantly, this calculation begins to break down when the effects of a realistic, finite width velocity distribution are properly accounted for; what we have done thus far is valid as long as

$$|\frac{\boldsymbol{k}\cdot\boldsymbol{V}}{k} - \frac{\omega}{k}| \gg w_i \text{ and } V_0 \gg w_e. \tag{II.65}$$

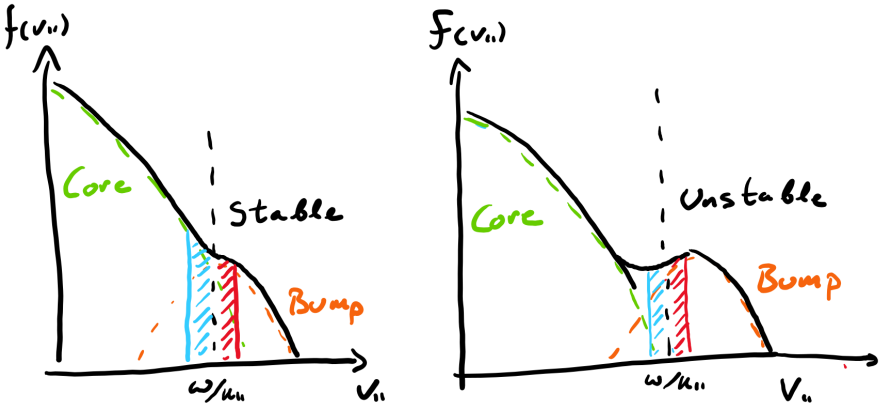

FIGURE 6. Two cases of the Bump-on-Tail distribution, one in which the beam is not sufficiently dense, cold, or fast to drive unstable waves (left) and one where a resonant instability occurs.

The fastest growing mode arises for

$$\omega \approx \omega_{pe}\left[1 + i\frac{\sqrt{3}}{2}\left(\frac{m_e}{2m_i}\right)^{1/3}\right]. \tag{II.66}$$

What is driving this instability? A straightforward interpretation is that of charge bunching. A local increase in the density of the electrons induces a change perturbation in a stream that passes over the bunch. Electrons passing over the bunch will be slowed down, and that slowing down will produce an increase in the local electron density, reinforcing the original clump. Thus an instability is formed.

II.3.3. *Bump-on-Tail Instability*

As was hinted at in the previous section, we need to develop a means of handling the effects of the thermal spread in velocity (the kinetic effects).

As a tractable test case, we consider the bump-on-tail distribution

$$\begin{aligned} F_e =& \frac{n_1}{n_e}\left(\frac{1}{w_{e1}}\right)^{3/2}\exp\left(-\frac{v^2}{w_{e1}}\right) + \frac{n_2}{n_e}\delta(v_x)\delta(v_y)\frac{1}{\sqrt{w_{e2}}} \\ &\times\frac{1}{2}\left\{\exp\left[-\frac{(v_z - V_0)^2}{w_{e2}^2}\right] + \exp\left[-\frac{(v_z + V_0)^2}{w_{e2}^2}\right]\right\} \end{aligned} \tag{II.67}$$

An analytic dispersion relation for a plasma with this distribution requires the use of the *Weak Growth Approximation*, where we will assume $\gamma \ll \omega$. Under this assumption, one can Taylor expand $D(\omega = (\omega_r, \gamma))$ about ω_0

$$\begin{aligned} D(\omega) &= D(\omega_0) + \gamma\frac{\partial D(\omega_0)}{\partial \omega} + \ldots \\ D(\omega) &= D(\omega_0) + \gamma\frac{\partial \omega_r}{\partial \omega}\frac{\partial D(\omega_0)}{\partial \omega_r} + \gamma\frac{\partial \gamma}{\partial \omega}\frac{\partial D(\omega_0)}{\partial \gamma} + \ldots \\ D(\omega) &= D(\omega_0) + i\gamma\frac{\partial D(\omega_0)}{\partial \omega_r}. \end{aligned} \tag{II.68}$$

Splitting D into its real and imaginary components, D_r and D_i (see Eqn. II.57 for the

general expressions), we can write (again, assuming $\gamma \ll \omega$)

$$D_r(\omega) = 0 \tag{II.69}$$

$$D_i(\omega) + \gamma \frac{\partial D_r(\omega_0)}{\partial \omega_r} = 0. \tag{II.70}$$

Manipulation of the imaginary component yields an expression for the growth rate

$$\gamma = \frac{-D_i(\omega)}{\frac{\partial D_r(\omega_0)}{\partial \omega_r}}. \tag{II.71}$$

Under the assumption that the wave phase speed is large compared to the thermal velocity $\omega/|k| \gg w_e$, and that $n_1 \gg n_2$, the real part of the frequency can be found

$$\omega_r^2 \approx \omega_{pe}^2 \left(1 + 3k^2\lambda_{D1}^2\right). \tag{II.72}$$

These frequencies are only very slightly different from those extracted from a single Maxwellian case. The imaginary component, however, can be quite different.

After some tedious algebra, one can find

$$\begin{aligned} \gamma \approx & -\sqrt{\frac{\pi}{8}} \frac{\omega_{p1}}{k^3\lambda_{D1}^3} \exp\left(-\frac{1}{2k^2\lambda_{D1}^2} - \frac{3}{2}\right) \\ & + \frac{n_2}{n_1}\left(\frac{T_1}{T_2}\right)^{3/2} \frac{k^3}{k_z^3}\left(\frac{k_z V_0}{\omega_r} - 1\right) \exp\left[-\frac{T_1/T_2}{2k_z^2\lambda_{D1}^2}\left(1 - \frac{k_z V_0}{\omega_r}\right)^2\right]. \end{aligned} \tag{II.73}$$

The first term is just Landau damping associated with the core distribution. It will always damp, and never contribute to the growth of an unstable wave. The second term is from the bump, and only velocities satisfying $\omega_r/k_z = v$ will resonant (we assumed the beam was cold in the $\hat{x}$ and $\hat{y}$ directions). If a wave has a phase velocity smaller than V_0, the mean velocity of the bump distribution, it can contribute to an unstable mode. For velocities larger than V_0, the bump will contribute to the damping of already driven by the core distribution. For any value of v, the damping or growth of a wave is determined by the local slope of F_e; if the bump is large enough to force the total distribution to have a positive slope, the distribution will be unstable to waves with phase speeds matching ω_r/k_z.

By inspection, the destabilizing contribution from the bump is greatest at $|k_z V_0|/\omega = 1 + \sqrt{k_z^2\lambda_{D1}^2 T_2/T_1}$. Evaluating the for the maximum growth rate at that wavenumber yields

$$\gamma_{\max} = \sqrt{\frac{\pi}{8}} \frac{\omega_{p1}}{k^3\lambda_{D1}^3}\left[\frac{n_2}{n_1}\left(\frac{T_1}{T_2}\right) k^3\lambda_{D1}^3 \frac{V_0^2}{w_{e1}^2} \exp\left(-\frac{1}{2}\right) - \exp\left(-\frac{1}{2k^2\lambda_{D1}^2} - \frac{3}{2}\right)\right]. \tag{II.74}$$

From this form, we see there are three ways to encourage unstable growth from the beam:

- Increase the number of beam particles (but not too much to invalidate the assumption $n_1 \gg n_2$).
- Make the beam more peaked (decrease T_2/T_1).
- Increase the bulk speed of the bump.

Generally, this kind of weak bump instability will always grow much more slowly than the two-stream instability.

II.3.4. *Nyquist Method and Penrose Criterion*

Can a more general means of determining the stability of a system be derived? In a word, yes.

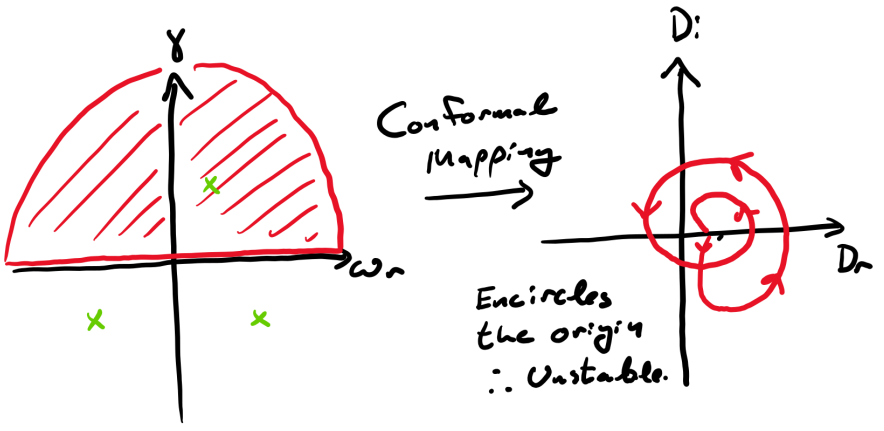

FIGURE 7. A schematic of the contour integral and the conformal mapping used to determine stability for the Nyquist method.

We already have convinced ourselves that a monotonically decreasing, isotropic function is stable, and have identified two cases where departures from that ideal state lead to the growth of unstable modes.

In his time at Bell Labs, Nyquist developed a very general method for determining the stability of electric circuits against feedback(Nyquist 1932). Physicists aware of this method adopted it the systems of equations governing plasmas, and in time produced a simplified version (Penrose 1960).

This method depends on the fact that question of stability depends on determining if $D(\omega, \boldsymbol{k}) = 0$ has any solutions with $\mathcal{I}(\omega) = \gamma > 0$. If such solutions exist, then the system is unstable. Seizing on this mathematical statement, Nyquist stated that if one were to perform a contour integral of D^{-1} over the upper half complex plane, illustrated in red in the right hand panel of Fig. 7, the complex frequency solutions that satisfy $D(\omega, \boldsymbol{k}) = 0$ would be poles, and thus could be counted by an application of the residue theorem

$$\frac{1}{2\pi i} \oint \frac{d\omega}{D(\omega, \boldsymbol{k})} \frac{\partial D}{\partial \omega} = W_n \tag{II.75}$$

where W_n is the number of poles in the upper half complex plane, which corresponds to the number of unstable modes associated with the chosen plasma equilibrium, as the function $\frac{1}{D(\omega,\boldsymbol{k})} \frac{\partial D}{\partial \omega}$ has been constructed to have poles wherever D has zeros.

One way to visualize this integration is perform a conformal mapping of the value of $D(\omega)$ over the real ω axis from $\omega \to -\infty$ to $\omega \to \infty$. Such a mapping is illustrated in the right hand panel of Fig. 7. One can show, with sufficient patience or a reading of section 9.6 of Krall and Trivelpiece (1973), that the number of times this contour encircles the origin is equal to W_n.

As a simple example of this mapping, let's consider the case of a monotonically decreasing $F(v)$ with a peak at v_0, which we know to be stable. Returning to Eqn. II.57, we take advantage of the fact that $dH(x)/dy \equiv 0$ to rewrite the integral

$$\int_{-\infty}^{\infty} \frac{dF(v)/dv}{v - \omega/|k|} dv = \int_{-\infty}^{\infty} \frac{d\left[F(v) - F(\omega/|k|)\right]/dv}{v - \omega/|k|} dv. \tag{II.76}$$

We also will need to use the *Plemelj Relation* to simplify the imaginary component of

D. This relation states

$$\lim_{\epsilon\to 0}\int_{-\infty}^{\infty} dx \frac{f(x)}{x-(x_0\pm i\epsilon)} = P\int_{-\infty}^{\infty} dx\frac{f(x)}{x-x_0} \pm i\pi f(x_0). \tag{II.77}$$

The real and imaginary components of the dielectric can thus be written, for real ω, ω, as

$$D_r = 1-\frac{\omega_{pe}}{k^2}\int_{-\infty}^{\infty} dv \frac{\partial F(v)-F(\omega/|k|)}{(v-\omega_r/|k|)^2} \tag{II.78}$$

$$D_i = -\pi\frac{\omega_{pe}^2}{k^2}\frac{\partial F}{\partial v}|_{v=\omega/|k|}. \tag{II.79}$$

From inspection, $D_i = 0$ for three values of ω, $-\infty, |k|v_0$. We can inspect the sign of D_r for these three frequencies. For $\omega = \pm\infty$, D_r is positive, with a value of 1 for $-\infty$ and $e^{2\pi i W_n}$ for ∞. At the peak v_0

$$D_r(\omega = |k|v_0) = 1+\frac{\omega_{pe}}{k^2}\int_{-\infty}^{\infty} dv\frac{\partial F(v_0)-F(v)}{(v-\omega_r/|k|)^2} > 0. \tag{II.80}$$

This last inequality holds as F has a maximum at v_0, and thus $F(v_0)-F(v) \geqslant 0\forall v$. Therefore, D_r is positive at all points where D_i vanishes, allowing us to construct the Nyquist diagram; see the bottom panel of Fig. 8. As the curve does not encircle the origin, there are no unstable modes.

Let's try a less trivial case, with a generic distribution with one minimum, at v_0, and two maxima, v_1 and v_2, with $F(v_1) > F(v_2)$. We can immediately write down the five frequencies at which D_i will be zero, $\omega = \pm\infty$, $|k|v_0$, $|k|v_1$, and $|k|v_2$. As before, we know that $D_r(\omega\to\pm\infty)$ and $D_r(\omega = |k|v_1)$ will be positive. The signs of D_r at the other two key frequencies will determine the stability of the plasma. While the exact values of D_r for $\omega = |k|v_0$ and $\omega = |k|v_2$ depend on the structure of F, we can state that $D_r(\omega = |k|v_0) < D_r(\omega = |k|v_2)$. More generally, if $D_r(\omega = |k|v) > 0$, the plasma is stable. This can be expressed mathematically as *the Penrose Criterion*:

$$P(F) = \int_{-\infty}^{\infty}\frac{F(v_0)-F(v)}{(v-v_0)^2}dv < 0. \tag{II.81}$$

If $P(F) < 0$, there must be some value of k for which $D_r(|k|u_2) > 0$ and $D_r(|k|u_0) < 0$. Even more usefully, the range of unstable wavevectors can be determined using

$$\omega_{pe}^2\int_{-\infty}^{\infty}\frac{F(v_2)-F(v)}{(v-v_2)^2}dv < k^2 < \omega_{pe}^2\int_{-\infty}^{\infty}\frac{F(v_0)-F(v)}{(v-v_0)^2}dv. \tag{II.82}$$

An important caveats: The Penrose criterion is a necessary and sufficient condition for *electrostatic* instabilities. It does not determine if *electromagnetic* waves can be driven. The more general Nyquist method can be used for both electrostatic and electromagnetic instabilities.[13]

Quoting Krall and Trivelpiece (1973)

> The Nyquist method is a powerful tool with which to study plasma stability because it makes it possible to predict stability by calculating the sign of D_r for a few particular values of ω_r rather than having to solve the equation $D = 0$.

[13]See Klein et al. (2017) for a discussion of an automated, numerical implementation of the Nyquist method.

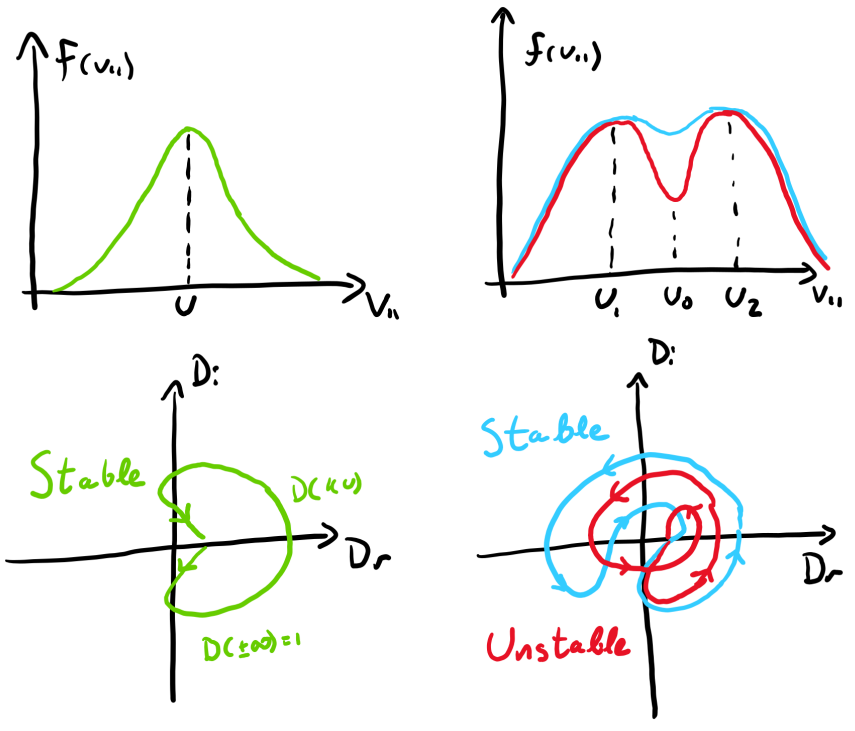

FIGURE 8. An application of the Nyquist method to a stable, monotonically decreasing function (left), as well as to a stable and unstable two-humped distribution.

II.3.4.1. *Weibel Instability*

Instead of being driven by multiple components, instabilities can also be driven by anisotropies in the velocity distribution.[14] The Weibel instability is such an example instability.

As a simple physical model, let's assume the ions are a fixed, immobile background and that the electrons are hotter in the $\hat{y}$ direction; effectively $T_y > T_x$ or T_z; this system is sketched in Fig. 9. In this setup, there are equal numbers of forward and backward propagating in the hot ($\hat{y}$) direction, so there is no net current induced by the equilibrium distribution.

Let us now introduce a small magnetic fluctuation, rising from the noise, in the $\hat{z}$ direction. For simplicity, this small fluctuation will be sinusoidal $\delta B_z = B_z \sin(kx)$. This initially small fluctuation will perturb the motion of the electrons, via the $\boldsymbol{v} \times \boldsymbol{B}$ component of the Lorentz force. The initially straight paths of the electrons will be diverted, from the dashed to the solid lines in Fig. 9. These diversions of electrons will act to create streams of downward or upward moving electrons, depending on the phase of the δB_z fluctuation. Streams of charged particles produce a current $\boldsymbol{j} = q_e n_e \boldsymbol{v}_e$ in the $\pm\hat{y}$ direction. This current in turn reinforces the initial magnetic fluctuation, strengthening the Lorentz force and further enhancing the current channels.

An analogy can be drawn to the two stream instability, but instead of electrostatic

[14]But what about Gardner? That proof by contradiction only applied to an monotonically decreasing, isotropic distribution. If the distribution is not isotropic, the plasma can be unstable.

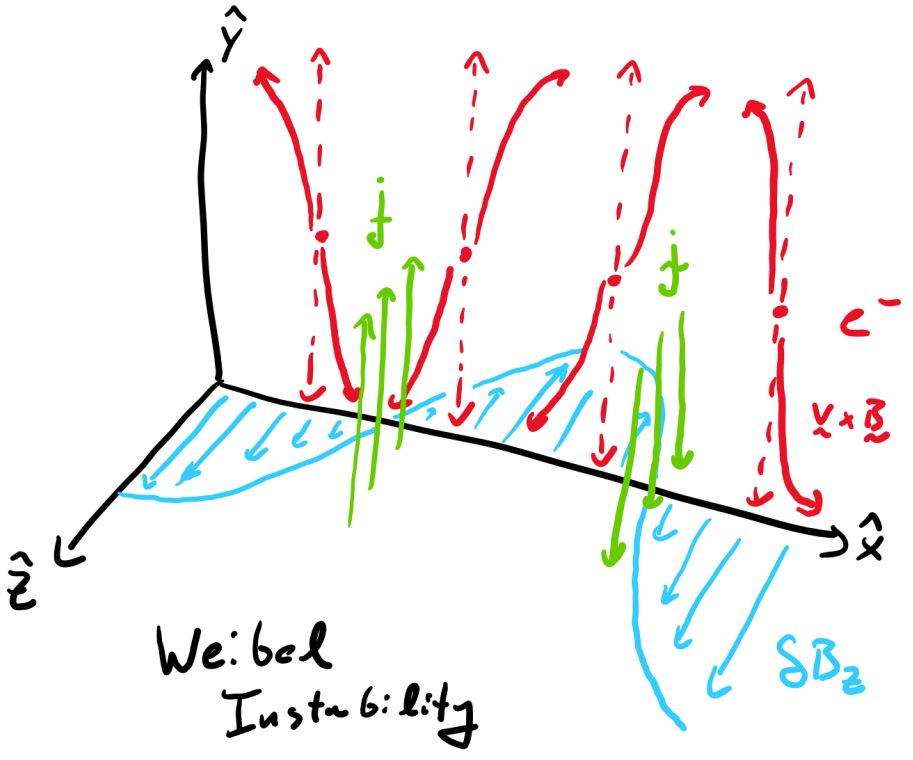

FIGURE 9. A schematic of the Weibel instability.

perturbations reinforced by spatial bunches of charge, electromagnetic perturbations are reinforced by filaments of current.

Unsurprisingly, this problem can be treated in a much more sophisticated fashion. We leave the maths to the enterprising student[15] and state by fiat that a linearization of electromagnetic fluctuations in an electrostatic systems

$$\frac{\partial \delta f_s}{\partial t} + i\boldsymbol{k}\cdot\boldsymbol{v}\delta f_s + \frac{q_s}{m_s}\left(\delta\boldsymbol{E} + \frac{\boldsymbol{v}\times\boldsymbol{B}}{c}\right)\cdot\frac{\partial F_s(\boldsymbol{v})}{\partial \boldsymbol{v}} = 0 \tag{II.83}$$

combined with a bi-Maxwellian distribution of electrons

$$F_e = \frac{n_{0s}}{\pi^{3/2} w_{\parallel,e} w_{\perp,e}^2}\exp\left(-\frac{v^2}{w_{\parallel,e'}^2} - \frac{v^2}{w_{\perp,e'}^2}\right) \tag{II.84}$$

yields a growth rate of

$$\gamma = \frac{k w_{\parallel,e}}{\sqrt{\pi}}\frac{T_{\parallel,e}}{T_{\perp,e}}\left(\frac{T_{\perp,e}}{T_{\parallel,e}} - 1 - k^2 d_e^2\right). \tag{II.85}$$

The Weibel instability is commonly invoked to arise in astrophysical plasma systems, including in collisionless shocks around supernova remnants and magnetogenesis.

[15] Questions 2 and 3 from the Plasma Kinetics Problem set found in http://www-thphys.physics.ox.ac.uk/people/AlexanderSchekochihin/KT/2015/KTLectureNotes.pdf can help to guide this derivation.

II.3.4.2. *Other Kinetic Instabilities*

There are a plethora of other kinds of kinetic instabilities that can arise in collisionless or weakly-collisional magnetized plasma systems. Some examples are the Alfvén Ion Cyclotron instability, which depends on the cyclotron rather than the Landau resonance, the mirror instability, which is driven by a difference in the response of particles with $v_\parallel \approx 0$ and the rest of the distribution to magnetic field fluctuations, and a family of firehose instabilities (fluid (Chew et al. 1956), parallel, and obliqueHellinger and Matsumoto (2000)), which depend on the presence of an excess parallel pressure. Details on most of these can be found in the excellent Gary (1993), with updates in Klein and Howes (2015) and Yoon (2017), or the table in Verscharen et al. (2019). The presence of the action of these instabilities in governing the evolution of the solar wind can be inferred from statistical observations (Kasper et al. 2002; Bale et al. 2009) as well as measurements of wavestorms (Jian et al. 2009; Gary et al. 2016); more recently, patches of waves observed near the Sun, (e.g. Verniero et al. 2020; Bowen et al. 2020; Klein et al. 2021) are also likely driven by these kinds of kinetic instabilities.

Takeaway Points:

- Departures from a Maxwellian velocity space distribution is a source of free energy that can, under certain circumstances, lead the generation of waves that act to move the system toward Maxwellianity.
- Typical features that can drive instabilities are beams (either cold or hot) or anisotropies in the velocity distribution.
- A number of tools are available to determine the stability of a system. Most require some familiarity with complex analysis.
- The wave modes associated with these instabilities are frequently observed in weakly collisional systems.

REFERENCES

Arfken, G., Weber, H. and Harris, F. 2013 *Mathematical Methods for Physicists: A Comprehensive Guide*. Elsevier Science. URL https://books.google.com/books?id=qLFo_Z-PoGIC.

Armstrong, J. W., Rickett, B. J. and Spangler, S. R. 1995 *Astrophys. J.* **443**, 209.

Balbus, S. A. and Hawley, J. F. 1998 *Reviews of Modern Physics* **70**, 1.

Bale, S. D., Kasper, J. C., Howes, G. G., Quataert, E., Salem, C. and Sundkvist, D. 2009 *Phys. Rev. Lett.* **103**, 211101.

Batchelor, G. K. 1953 *The Theory of Homogeneous Turbulence*.

Boldyrev, S. 2006 *Phys. Rev. Lett.* **96**, 115002.

Bowen, T. A., Mallet, A., Huang, J., Klein, K. G., Malaspina, D. M., Stevens, M., Bale, S. D., Bonnell, J. W., Case, A. W., Chandran, B. D. G., Chaston, C. C., Chen, C. H. K., Dudok de Wit, T., Goetz, K., Harvey, P. R., Howes, G. G., Kasper, J. C., Korreck, K. E., Larson, D., Livi, R., MacDowall, R. J., McManus, M. D., Pulupa, M., Verniero, J. L. and Whittlesey, P. 2020 *Astrophys. J. Supp.* **246**, 66.

Brown, J. and Churchill, R. 2004 *Complex Variables and Applications* Brown-Churchill series. McGraw-Hill Higher Education. URL https://books.google.com/books?id=4vfuAAAAMAAJ.

Bruno, R. and Carbone, V. 2013 *Living Rev. Solar Phys.* **10**, 2.

Chen, C. H. K. 2016a *J. Plasma Phys.* **82**, 535820602.

Chen, C. H. K., Leung, L., Boldyrev, S., Maruca, B. A. and Bale, S. D. 2014 *Geophys. Res. Lett.* **41**, 8081.

Chen, F. F. 2016b *Introduction to Plasma Physics and Controlled Fusion*.

Chew, G. F., Goldberger, M. L. and Low, F. E. 1956 *Royal Society of London Proceedings Series A* **236**, 112.

Cranmer, S. R., van Ballegooijen, A. A. and Edgar, R. J. 2007 *Astrophys. J. Supp.* **171**, 520.

Dimits, A. M., Bateman, G., Beer, M. A., Cohen, B. I., Dorland, W., Hammett, G. W., Kim, C., Kinsey, J. E., Kotschenreuther, M., Kritz, A. H., Lao, L. L., Mand rekas, J., Nevins, W. M., Parker, S. E., Redd, A. J., Shumaker, D. E., Sydora, R. and Weiland, J. 2000 *Phys. Plasmas* **7**, 969.

Elsasser, W. M. 1950 *Phys. Rev.* **79**, 183.

Fried, B. D. and Conte, S. D. 1961 *The Plasma Dispersion Function*. Academic Press.

Frisch, U. 1995 *Turbulence*.

Galtier, S., Nazarenko, S. V., Newell, A. C. and Pouquet, A. 2000 *J. Plasma Phys.* **63**, 447.

Gary, S. P. 1993 *Theory of Space Plasma Microinstabilities*.

Gary, S. P., Jian, L. K., Broiles, T. W., Stevens, M. L., Podesta, J. J. and Kasper, J. C. 2016 *J. Geophys. Res.* **121**, 30.

Goldreich, P. and Sridhar, S. 1995 *Astrophys. J.* **438**, 763.

Goldreich, P. and Sridhar, S. 1997 *Astrophys. J.* **485**, 680.

Hellinger, P. and Matsumoto, H. 2000 *J. Geophys. Res.* **105**, 10519.

Iroshnikov, P. S. 1964 **7**, 566.

Jian, L. K., Russell, C. T., Luhmann, J. G., Strangeway, R. J., Leisner, J. S. and Galvin, A. B. 2009 *Astrophys. J. Lett.* **701**, L105.

Kasper, J. C., Lazarus, A. J. and Gary, S. P. 2002 *Geophys. Res. Lett.* **29**, 1839.

Kim, E.-J. 2005 *Astron. Astrophys.* **441**, 763.

Klein, K. G. and Howes, G. G. 2015 *Phys. Plasmas* **22**, 032903.

Klein, K. G., Kasper, J. C., Korreck, K. E. and Stevens, M. L. 2017 *Journal of Geophysical Research (Space Physics)* **122**, 9815.

Klein, K. G., Verniero, J. L., Alterman, B., Bale, S., Case, A., Kasper, J. C., Korreck, K., Larson, D., Lichko, E., Livi, R., McManus, M., Martinović, M., Rahmati, A., Stevens, M. and Whittlesey, P. 2021 *Astrophys. J.* **909**, 7.

Kolmogorov, A. 1941 *Akademiia Nauk SSSR Doklady* **30**, 301.

Kraichnan, R. H. 1965 *Phys. Fluids* **8**, 1385.

Krall, N. A. and Trivelpiece, A. W. 1973 *Principles of plasma physics*. McGraw-Hill.

Kunz, M. W., Stone, J. M. and Quataert, E. 2016 *Phys. Rev. Lett.* **117**, 235101.

Landau, L. D. 1946 *J. Phys.(USSR)* **10**, 25. [Zh. Eksp. Teor. Fiz.16,574(1946)].

Lithwick, Y. and Goldreich, P. 2003 *Astrophys. J.* **582**, 1220.

Lithwick, Y., Goldreich, P. and Sridhar, S. 2007 *Astrophys. J.* **655**, 269.

Loureiro, N. F. and Boldyrev, S. 2017 *Phys. Rev. Lett.* **118**, 245101.

Mallet, A., Schekochihin, A. A. and Chandran, B. D. G. 2015 *Mon. Not. Roy. Astron. Soc.* **449**, L77.

Mallet, A., Schekochihin, A. A. and Chandran, B. D. G. 2017 *Mon. Not. Roy. Astron. Soc.* **468**, 4862.

Montgomery, D. and Matthaeus, W. H. 1995 *Astrophys. J.* **447**, 706.

Ng, C. S. and Bhattacharjee, A. 1996 *Astrophys. J.* **465**, 845.

Nicholson, D. 1983 *Introduction to plasma theory* Wiley series in plasma physics. Wiley. URL https://books.google.com/books?id=fyRRAAAAMAAJ.

Nyquist, H. 1932 *Bell system technical journal* **11**, 126.

Penrose, O. 1960 *Physics of Fluids* **3**, 258.

Schekochihin, A. A. 2020 *arXiv e-prints* arXiv:2010.00699.

Shebalin, J. V., Matthaeus, W. H. and Montgomery, D. 1983 *J. Plasma Phys.* **29**, 525.

Sridhar, S. and Goldreich, P. 1994 *Astrophys. J.* **432**, 612.

Stix, T. H. 1992 *Waves in plasmas*. American Institute of Physics.

Verniero, J. L., Larson, D. E., Livi, R., Rahmati, A., McManus, M. D., Pyakurel, P. S., Klein, K. G., Bowen, T. A., Bonnell, J. W., Alterman, B. L., Whittlesey, P. L., Malaspina, D. M., Bale, S. D., Kasper, J. C., Case, A. W., Goetz, K., Harvey, P. R., Korreck, K. E., MacDowall, R. J., Pulupa, M., Stevens, M. L. and de Wit, T. D. 2020 *Astrophys. J. Supp.* **248**, 5.

Verscharen, D., Klein, K. G. and Maruca, B. A. 2019 *Living Rev. Solar Phys.* **16**, 5.

Vlasov, A. 1945 *J. Phys.(USSR)* **9**, 25.

Yoon, P. H. 2017 *Reviews of Modern Plasma Physics* **1**, 4.

Zhuravleva, I., Churazov, E., Schekochihin, A. A., Allen, S. W., Arévalo, P., Fabian, A. C., Forman, W. R., Sanders, J. S., Simionescu, A., Sunyaev, R., Vikhlinin, A. and Werner, N. 2014 *Nature* **515**, 85.